REPUBLIC OF TURKEY
YILDIZ TECHNICAL UNIVERSITY
GRADUATE SCHOOL OF SCIENCE AND ENGINEERING

GRAPHENE REINFORCED NANOCOMPOSITES: MANUFACTURING AND CHARACTERIZATION

Besim Emre BİRKAN

MASTER OF SCIENCE THESIS
Department of Mechanical Engineering
Construction MSc. Program

Supervisor
Asst. Prof. Alperen ACAR

January, 2022

REPUBLIC OF TURKEY
YILDIZ TECHNICAL UNIVERSITY
GRADUATE SCHOOL OF SCIENCE AND ENGINEERING

GRAPHENE REINFORCED NANOCOMPOSITES: MANUFACTURING AND CHARACTERIZATION

A thesis submitted by Besim Emre BİRKAN in partial fulfillment of the requirements for the degree of **MASTER OF SCIENCE** is approved by the committee on 17.01.2022 in Department of Mechanical Engineering, Construction MSc. Program.

Asst. Prof. Alperen ACAR
Yildiz Technical University
Supervisor

Approved By the Examining Committee

Asst. Prof. Alperen ACAR, Supervisor
Yildiz Technical University _____

Prof. Dr. Özgen ÇOLAK ÇAKIR, Member
Yildiz Technical University _____

Asst. Prof. Özge ÖZDEMİR , Member
Istanbul Technical University _____

I hereby declare that I have obtained the required legal permissions during data collection and exploitation procedures, that I have made the in-text citations and cited the references properly, that I haven't falsified and/or fabricated research data and results of the study and that I have abided by the principles of the scientific research and ethics during my Thesis Study under the title of Graphene Reinforced Nanocomposites: Manufacturing and Characterization supervised by my supervisor, Asst. Prof. Alperen ACAR. In the case of a discovery of false statement, I am to acknowledge any legal consequence.

Besim Emre BİRKAN

Signature

This study was supported by the Scientific and Technological Research Council of Turkey (TUBITAK) Grant No: 119M088.

Dedicated to my family
and Bade

ACKNOWLEDGEMENTS

I would like to thank esteemed Prof. Dr. Özgen ÇOLAK ÇAKIR, who helped me start this work by including me in her project and did not spare her help and knowledge throughout my work. I would like to thank my advisor, Asst. Prof. Alperen ACAR, whose knowledge and support I always felt by my side. I would like to thank my dear colleague Okan BAKBAK, who supported me throughout the whole process. I would also like to thank the staff of YTU Central Laboratory and Beril GÜMÜŞ, who helped me benefit from the testing facilities. This thesis work was supported by Scientific and Technological Research Council of Turkey TUBITAK (Grand No: 119M088). I would like to thank TUBITAK for its contributions and support.

Besim Emre BİRKAN

TABLE OF CONTENTS

LIST OF SYMBOLS viii

LIST OF ABBREVIATIONS ix

LIST OF FIGURES x

LIST OF TABLES xii

ABSTRACT xiii

ÖZET xv

1 INTRODUCTION 1

1.1 Literature Review 1

1.1.1 Carbon Based Nanomaterials 1

1.1.2 Graphene Fabrication Methods 2

1.1.3 Properties of Epoxy Resins 3

1.1.4 Manufacturing of Epoxy Based-Graphene Filled Nano-composite Materials 5

1.2 Objective of the Thesis 7

1.3 Hypothesis 7

2 MANUFACTURING OF GRAPHANE-EPOXY NANOCOMPOSITES 8

2.1 Manufacturing of Pure Epoxy Specimens 8

2.1.1 Developing The Mold to be Used in Specimen Manufacturing by Soft Molding Method 8

2.1.2 Steps of Production For Pure Epoxy Specimens 10

2.2 Manufacturing of Graphene-Epoxy Specimens 12

2.2.1 Three Roll Milling Method 14

2.2.2 Functionalization of Graphene 15

2.2.3 Nanocomposite Production 17

3 CHARACTERIZATION OF GRAPHENE-EPOXY NANOCOMPOSITES 19

3.1 ARALDITE LY564 Epoxy Compression Test Results 19

3.2 f-GNF - Epoxy Nano-composite Compressive Test Results 23
3.2.1 Determining the Optimum Number of Cycles in 3RM 23
3.2.2 Compression Test Results for Functional Graphene - Epoxy Nano-composite Specimens 24

4 RESULTS AND DISCUSSIONS **31**

REFERENCES **34**

PUBLICATIONS FROM THE THESIS **39**

LIST OF SYMBOLS

Å	Angstrom
gr	Gram
h	Hour
K	Kelvin
kN	Kilonewton
MPa	Megapascal
m	Meter
ml	Milliliter
mm	Millimeter
min	Minute
nm	Nanometer
s	Second
SiC	Silicon Carbide
ϵ	Strain
σ	Stress
TPa	Terapascal
W	Watt
wt	Weight

LIST OF ABBREVIATIONS

CNT	Carbon Nanotubes
CVD	Chemical Vapor Doposition
CAE	Cycloaliphatic Epoxy Resin
DGEBA	Diglycidyl Ether Of Bisphenol-A
f-GNF	Functionalized Graphene
GIC	Graphene-intercalated Compounds
GO	Graphite Oxide
PMMA	Polymethyl methacrylate
PSS	Sodium 4-styrenesulfonate
3RM	Three Roll Milling
UV	Ultraviolet
YTU	Yıldız Technical University

LIST OF FIGURES

Figure 2.1 PMMA negative mold 9
Figure 2.2 Silicon mold prepared for compressive test specimens 9
Figure 2.3 Pure epoxy specimens obtained with the first method 11
Figure 2.4 Pure epoxy specimens after improvements 11
Figure 2.5 Pure epoxy specimens used in experiments 12
Figure 2.6 Technical drawing showing specimen dimensions 13
Figure 2.7 a) Three roll milling configuration, b) High shear region between the rolls 14
Figure 2.8 Exakt 80E Three Roll Mill device 15
Figure 2.9 Functionalization process of graphene 16
Figure 2.10 Production of nanocomposite specimens using 3RM 17
Figure 3.1 Compression test results at strain rate 1.E-3 /s for pure epoxy material (3 test repetitions) 19
Figure 3.2 Compression test results at strain rate 1.E-2 /s for pure epoxy material (3 test repetitions) 20
Figure 3.3 Compression test results at strain rate 1.E-1 /s for pure epoxy material (3 test repetitions) 20
Figure 3.4 True stress-strain response of pure epoxy (Araldite LY564) at three different strain rates (1.E-3, 1.E-2, 1.E-1 /s) 21
Figure 3.5 The true stress- strain curves under compression for specimens produced with different cycle numbers (Material: GNF- epoxy) . . 24
Figure 3.6 Compression tests of 0.1 wt% f-GNF-Epoxy nano-composites at 1.E-3 /s strain rate (3 test repetitions) 25
Figure 3.7 True stress-strain curves of f-GNF-epoxy nano-composites with f-GNF content of 0.1 wt% at three different strain rates) 26
Figure 3.8 True stress-strain curves of f-GNF-epoxy nano-composites with f-GNF content of 0.5 wt % under three different strain rates 27
Figure 3.9 Comparison of true stress-strain behaviors of f-GNF-epoxy nanocomposites with f-GNF content of 0.1 and 0.5 wt % with pure epoxy at 1.E-3 /s strain rate. 28

Figure 3.10 Comparison of true stress-strain behaviors of f-GNF-epoxy nanocomposites with f-GNF content of 0.1 and 0.5 wt % with pure epoxy at 1.E-2 /s strain rate. 29
Figure 3.11 Comparison of true stress-strain behaviors of f-GNF-epoxy nanocomposites with f-GNF content of 0.1 and 0.5 wt% with pure epoxy at 1.E-1 /s strain rate. 29

LIST OF TABLES

Table 3.1 The mechanical properties of Araldite LY 564 epoxy obtained from the quasi-static compression test 23
Table 3.2 The mechanical properties of Araldite LY 564 epoxy and f-GNF-epoxy nano-composite (0.1 and 0.5 wt% f-GNF) obtained from the quasi-static compression tests 27
Table 3.3 The increase in material properties as per centum for different graphene concentrations and strain rates. 28

ABSTRACT

Graphene Reinforced Nanocomposites: Manufacturing and Characterization

Besim Emre BİRKAN

Department of Mechanical Engineering
Master of Science Thesis

Supervisor: Asst. Prof. Alperen ACAR

The main problem encountered in the production of graphene reinforced nanocomposites is the agglomeration of graphene particles in the matrix material. Since the agglomerated graphene particles act as an impurity, not as a reinforcement element in the matrix material, a decrease is observed in the mechanical properties of the produced nano composite instead of an increase. In order to prevent this situation two strategies used, a three-roll milling device to disperse and Triton X-100 surfactant for functionalization were used in this study.

The properties that affect the mechanical properties of the nanocomposite produced, such as the roller speed and the distance between the rollers in the three-roll milling method, and the Triton X-100 ratio in the functionalization method, were determined by a detailed literature review.

After determining the production method, samples were produced at two different graphene ratios (0.1 and 0.5 wt%) and the effect of graphene ratio on mechanical properties was investigated. Since epoxy resin is a polymer material, it is also important to determine its time-dependent properties. For this reason, the viscoelastic and viscoplastic properties of the produced nanocomposites were determined by repeating the experiments at three different strain rates (1.E-3, 1.E-2 and 1.E-1 /s).

As a result, in this study, the optimum method for the production of graphene-epoxy nano-composites was determined and an improvement of up to 29% in elasticity modulus and up to 18% in yield strength was observed in nano-composite

specimens produced with this method, compared to pure epoxy specimens. The mechanical properties of nanocomposites were brought to the literature by performing compression tests at different strain rates on the specimens produced with different graphene percentages.

Keywords: Graphene, epoxy, nanocomposite, functionalization, three roll milling

ÖZET

Grafen Takviyeli Nanokompozitler: Üretim ve Karakterizasyon

Besim Emre BİRKAN

Makine Mühendisliği Anabilim Dalı
Yüksek Lisans Tezi

Danışman: Dr. Öğr. Üyesi Alperen ACAR

Grafen takviyeli nanokompozit üretiminde karşılaşılan başlıca sorun grafen partiküllerinin matris malzemesi içerisinde topaklanmasıdır. Topaklanan grafen partikülleri matris içerisinde takviye elamanı olarak değil bir safsızlık gibi davranış gösterdiğinden üretilen nanokompozitin mekanik özelliklerinde artış yerine azalma gözlemlenmektedir. Bu durumun önlenmesi amacı ile bu çalışmada üç merdaneli hadde cihazı ve Triton X-100 yüzey aktif maddesi kullanılmıştır.

Üç merdaneli hadde yönteminde merdane hızı ve merdaneler arası mesafe, fonksiyonelleştirme yönteminde de Triton X-100 oranı gibi üretilen nanokompozitin mekanik özelliklerine etkisi olan özellikler detaylı literatür taraması yapılarak belirlenmiştir.

Üretim yönteminin belirlenmesinden sonra iki farklı grafen oranında (kütlece %0,1 ve %0,5) numuneler üretilmiş ve grafen oranının mekanik özelliklere etkisi incelenmiştir. Epoksi reçine polimer malzeme olduğundan zamana bağımlı özelliklerinin belirlenmesi de önem arz etmektedir. Bu nedenle yapılan deneyler üç farklı şekil değiştirme hızında (1.E-3, 1.E-2 ve 1.E-1 /s) tekrarlanarak üretilen nanokompozitlerin viskoelastik ve viskoplastik özellikleri belirlenmiştir.

Sonuç olarak bu çalışmada grafen-epoksi nanokompozitlerin üretilmesinde optimum yöntem belirlenmiş ve bu yöntem ile üretilmiş nanokompozit numunelerde saf epoksi numunelere göre elastisite modülünde %29'a, akma dayanımında is %18'e kadar bir iyileşme gözlemlenmiştir. Farklı grafen yüzdeleri ile üretilen numunelere farklı şekil

değiştirme hızlarında basma testleri yapılarak nanokompozitlerin mekanik özellikleri literatüre kazandırılmıştır.

Anahtar Kelimeler: Grafen, epoksi, nanokompozit, fonksiyonelleştirme, üç merdaneli hadde

1
INTRODUCTION

1.1 Literature Review

1.1.1 Carbon Based Nanomaterials

Nanomaterials are defined as material with any dimension in the nanoscale (length range approximately from 1 to 100 nanometers(nm)). Family of carbon-based nanomaterials such as graphene, carbon nanotubes, carbon nanofibers, etc. are considered most important in the literature due to their superiority in the fields of mechanical, thermal, and electrical properties.

Graphene is the most conspicuous member of this family due to its form of a two-dimensional sheet of carbon atoms and its excellent physical, thermal, and electrical properties. Graphene is also the strongest material ever tested with an elasticity modulus of 1 TPa. A single layer of graphenes thermal conductivity is measured by Balandin et al. as 3080–5150 W/mK [1]. These properties of graphene make it an excellent candidate for use as a filler for epoxy-based nanocomposites.

Carbon nanotubes(CNT) are one atom thick layer of graphene sheets rolled up as a tubular shell. This property causes CNTs to be one-dimensional and have a large geometric aspect ratio. Due to their C-C covalent bonding and hexagonal structure CNTs show excellent mechanical, electrical, and thermal properties. In their axial orientation, CNTs have an extremely high Young modulus. Because of its length, the nanotube as a whole is extremely flexible. As a result, these compounds may be acceptable for use in composite materials that require anisotropic characteristics.

Carbon nanofiber consist of the graphite sheet completely arranged in various orientations [2]. One of the most striking characteristics of these structures is the abundance of sides, which creates sites for chemical or physical interaction, particularly adsorption. Carbon nanofibers are available in lengths ranging from 5 to several hundred microns and diameters ranging from 100 to 300 nm.

1.1.2 Graphene Fabrication Methods

Several graphene fabrication methods developed since its discovery by Novoselov et. al in 2004. Novoselov et al used sticky tape to successfully isolate a layer from graphite to obtain a single atom thick 2D allotrope of carbon which is graphene [3]. This method and other mechanical exfoliation methods requires an external force of 300 $nN/\mu m^2$ to separate one layer of graphene from graphite [4]. There are various methods for accomplishing mechanical exfoliation like sticky tape [3] , electric field [5] , and ultrasonication [6]. However, the problem with the mechanical exfoliation method is its lack of scalability and reproducibility.

At low temperatures, the chemical exfoliation process is utilized to synthesize a large amount of graphene. This method involves adding alkali metals to the graphite solution. Alkali metals with their relatively small atomic radius get into layers between graphite and therefore weaken the van der Waals bonds between the graphite layers. This chemical reaction causes the formation of graphene-intercalated compounds (GIC). GICs were then dispersed inside a liquid medium using sonication to produce graphene. The problem with this method is the quick reassembly of graphene to graphite after the fabrication process [7].

Another method to use for producing graphene in large amounts is the chemical synthesis method. The method works with the principle of reducing graphite to graphite oxide(GO) with strong acids. When graphite turns into GO interlayer spacing between graphene sheets increases up to four times their initial distance between them. With prolonged oxidation time this distance can raise to 7.35 Å [8]. Lastly with the hydrazine hydrate treatment GO reduces to graphene. The requirement of toxic chemicals and observed defects in the graphene produced using this method are two main problems that have led researchers to seek new graphene production methods.

All three of these methods are referred to as top-down methods in the literature meaning these methods are used graphite to obtain graphene. Other than these methods graphene can be fabricated by atomic or molecular rearrangement of carbon. These methods are named bottom-up methods in general. One of these methods is the pyrolysis of graphene. With a 1:1 molar ratio of ethanol and sodium, this reaction is carried out in a closed vessel under high pressure. Graphene sheets can be smoothly separated by pyrolysis of sodium ethoxide using sonication [9].

One of the most well-known synthesis procedures is the epitaxial thermal synthesis of graphene on the surface of single-crystalline silicon carbide (SiC). The term "epitaxy" refers to a technique that allows a single-crystalline film (epitaxial film) to be deposited

on a single-crystal substrate. A homoepitaxial layer is generated when the epitaxial film and the substrate are made of the same material, while a heteroepitaxial film is formed when the epitaxial film and the substrate are made of different materials. Epitaxial growth on SiC produces a single-layer graphite or graphene heteroepitaxial layer [10]. Because of its scalability, superior electrical characteristics, and especially high-quality graphene, epitaxial development of graphene on SiC is very promising.

Thermal chemical vapor deposition(CVD) of graphene works with the principle of the flow of gases like methane, hydrogen, and argon in specific ratios into a quartz tube that contains a substrate such as Cu at high temperatures in a furnace is used to make graphene. Graphene is deposited in single, bilayer, or multilayer layers over time, depending on predefined circumstances like reaction time, gas flow rate, temperature, and pressure. The CVD approach has largely been used to generate graphene on Cu and Ni substrates. However, the time-consuming non-self-limiting growth of graphene on Ni substrate, as well as the formation of a significant number of folds and wrinkles, were both issues. Copper substrates have shown to be more conducive to graphene CVD development [11–13].

Arc discharge of graphite, and electron beam irradiation of PMMA nanofibers are some of the various ways to manufacture graphene [14–16]. The synthesis of boron- and nitrogen-doped graphene is also widely conducted using arc discharge techniques [17, 18].

1.1.3 Properties of Epoxy Resins

Because of its remarkable mechanical qualities, strong adhesion, superior heat and electrical resistance, epoxy resins have been widely employed for coatings, electronic materials, adhesives, and matrices for fiber-reinforced composites. The type of epoxy resin, hardener, and curing method all influence the final qualities of cured epoxy resins.

1.1.3.1 Types of Epoxy Resins

Bisphenol-A epoxy resins: Epichlorohydrin reacts with bisphenol-A in the presence of a basic catalyst to form the diglycidyl ether of bisphenol-A (DGEBA). The number of repeating units determines the qualities of the DGEBA resin.Molecules that have low molecular weight are fluids, whereas Molecules that have higher molecular weight are viscous liquids or solids [19, 20].

Cycloaliphatic epoxy resins: 3',4'-epoxycyclohexyl-methyl

3,4-epoxycyclohexanecarboxylate, a cycloaliphatic epoxy resin (CAE), is made by reacting 3'-cyclohexenylmethyl 3-cyclohexenecarboxylate with peracetic acid. This epoxy resin contains a fully saturated molecular structure and an aliphatic backbone, which contribute to its high UV stability, weatherability, thermal stability, and electrical properties. These characteristics are critical for resins utilized in the fabrication of structural components that must be used in high-temperature environments [21, 22].

Trifunctional epoxy resins: Trimethylol propane-N-triglycidyl ether, a trifunctional epoxy resin, can be made by reacting trimethylol propane with epichlorohydrin. This epoxy resin is a non-crystalline, low-viscosity plastic that may be cured at low temperatures [23, 24].

Tetrafunctional epoxy resins: Epichlorohydrin is used to make tetrafunctional epoxy resins by reacting 1,3-diaminobenzene or 4,4'-aminodiphenyl methane with epichlorohydrin. Because of their high functionality and density of crosslinking , these epoxy resins are utilized in operations requiring great temperature tolerance. The cured epoxy resins have strong chemical resistance, high modulus, UV blocking ability, and thermal stability [25].

Novolac epoxy resins: Glycidyl ethers of phenolic novolac resins have been made by reacting phenolic novolac resin with epichlorohydrin to produce novolac epoxy resins. Novolac epoxy resins' numerous epoxide groups contribute to their high cross-linking densities, which result in exceptional heat, chemical, and solvent resistance [26].

Biobased epoxy resins: Because of their low cost and biodegradability, polymers generated from renewable natural resources such as proteins, carbohydrates, starch, and lipids have piqued attention. Vegetable oils are multi-component combinations of various triacylglycerols, or glycerol and, fatty acid esters. Organic peracids or H_2O_2 may easily epoxidize triglycerides with a wide range of unsaturation sites, and epoxidized vegetable oils have a lot of potential as low-cost, renewable materials for industrial uses [27, 28].

Phosphorus-containing epoxy resins: Through flame inhibition in the gas phase and char amplification in the condensed phase, phosphorus compounds could offer a strong flame-retardant character to epoxy resins. In comparison to halogen-containing chemicals, they also produce less hazardous gas and smoke. Phosphorus-containing oxirane compounds could be used to incorporate covalently attached phosphorus into epoxy resins [29, 30].

1.1.3.2 Application Fields of Epoxy Resins

Paints and coatings: Because of their exceptional properties, such as ease of processing, high safety, excellent solvent and chemical resistance, toughness, low shrinkage on cure, mechanical and corrosion resistance, and excellent adhesion to a variety of substrates, epoxy resins are widely used as heavy-duty anti-corrosion coatings. Epoxy resins are frequently used to coat metal cans and containers to avoid rusting, especially when packing acidic foods like tomatoes. [31, 32].

Adhesives: Epoxy adhesives are a prominent component of the "structural adhesives" category of adhesives. These high-performance adhesives are utilized in the manufacture of aircraft, automobiles, bicycles, boats, and other items that demand strong bonding. It is vital to maximizing the shear strength of epoxy at both cryogenic and ambient temperatures when utilized as adhesives in cryogenic engineering applications.To boost adhesive strength and stimulate chemical interaction at the substrate/adhesive contact, the adhesives are typically cured at high temperatures [33, 34].

Industrial tooling: In industrial tooling applications, epoxy systems are used to create molds, master models, castings, fittings, and other industrial production aids. This applications substitutes materials like metal and wood in many industrial processes, improving process efficiency while lowering overall costs. Metallic components and tubular pipes have been successfully repaired using fiber-reinforced epoxy composites. In hydrogen storage cylinders, the composites also serve as load-bearing units [35].

Aerospace industry: Because of their great adhesive characteristics and low cost, epoxy resins have been widely used for structural adhesive applications in the aerospace sector. Epoxy resins reinforced with high-strength glass, carbon, Kevlar, or boron fibers have the most application potential in aircraft [36].

1.1.4 Manufacturing of Epoxy Based-Graphene Filled Nano-composite Materials

The dispersion of Nano filler is the most important phase in all Nano-composite production techniques. A well-distributed composite structure guarantees that the contact area between the matrix and the filler is maximized. As a result, a successful load transfer from matrix to filler will be realized from a molecular standpoint. It is well known that all nanofillers, including graphene, have a considerable agglomeration tendency. As a result, the majority of efforts in creating nanocomposites fabrication processes have focused on achieving a homogeneous and well-distributed composite structure.

In order to achieve good dispersion to prevent agglomerations several methods take place in the literature:

- Solution Mixing
- Melt Mixing
- In-situ Polymerization

1.1.4.1 Solution Mixing

For the creation of polymer-graphene nanocomposites, solution mixing is the most prevalent approach. Three steps make up the solution mixing process [37, 38]:

- The first step is to use ultrasonication to disperse graphene in an appropriate solvent.
- Following that, the polymer is added to an ultrasonicated graphene and solvent mixture.
- Entire mixture stirred to achieve improved graphene dispersion inside the polymer matrix.
- The final stage comprises removing the solvent via evaporation which affects the quality of the polymer-graphene nanocomposite created on a solid substrate, as well as the overall mixing efficiency and solvent suitability.

Many investigations on the fabrication of polymer-graphene nanocomposites using various graphene fillers and polymer mixtures have been conducted. The solution mixing approach is widely used in the creation of polymer-graphene nanocomposites. However, this process has a number of drawbacks, including the use of toxic solvents for dispersion, a low yield, and a high cost, making it unsuitable for commercial manufacture of polymer-graphene nanocomposites.

1.1.4.2 Melt Mixing

In comparison to the solution mixing method, melt mixing is a practical, neat, environmentally friendly, and diverse methodology. For mixing the polymer matrix with graphene fillers, the melt mixing approach does not require the use of a solvent, but the solution mixing method requires. By subjecting shear force to the polymer matrix and graphene, melt mixing works on the idea of physical mixing. Melt mixing

is done with extruders, kneaders, calenders, or other similar machines, and this approach is usually suitable for fabricating thermoplastic polymers. The use of high temperatures softens the matrix material, allowing for better graphene filler dispersion in the mixture. Furthermore, the main benefits of melt mixing can be linked to the procedure's cost-effectiveness and the ability to process vast quantities of materials [39, 40].

1.1.4.3 In Situ Polymerization

For the creation of nanocomposites, in situ polymerization is a unique and extremely successful approach. When compared to alternative production methods, this method allows for better filler dispersion inside matrix material. The separation of monomers and fillers in a solvent by mixing or sonication, is required for the creation of polymer-graphene nanocomposites. When an extra curing agent is added to a monomer solution containing well-dispersed fillers, the polymerization process begins, eventually leading to the creation of polymer-graphene nanocomposites The disadvantage of this approach is that it polymerizes monomers without any graphene, resulting polymerization rates to reduce [41].

1.2 Objective of the Thesis

In this study, it is aimed to develop the optimum method to be used in the manufacturing of graphene-epoxy nanocomposite and to make the mechanical characterization of the nanocomposites produced with this developed method. For this, the 3RM device and the functionalization of graphene were used as a hybrid in the production of materials and compression tests were performed on the specimens produced with different graphene ratios at different strain rates.

1.3 Hypothesis

Observing that there will be an improvement in the mechanical properties of nanocomposite specimens produced with the manufacturing method in which 3RM and graphene functionalization methods are used as hybrid.

2
MANUFACTURING OF GRAPHANE-EPOXY NANOCOMPOSITES

Well dispersed reinforcing agent ensures improvement in material properties for emerging nanocomposites. It is equally important to develop a reliable process to produce nanocomposites as well as choosing the best method for dispersion.

2.1 Manufacturing of Pure Epoxy Specimens

With the intention of observing improvements adding graphene makes inside the matrix material, first pure epoxy specimens are manufactured as a control group. The epoxy system has chosen to be Araldite LY564/ Aradur 2954 supplied by HUNTSMAN to produce pure epoxy specimens as well as using it as a matrix material for manufacturing nanocomposites for all specimens experiments conducted with. This epoxy system is widely used in industries such as automotive, aviation, ballistics, and armor. These industries' requirements for detailed material properties for this epoxy system are played a big role when deciding what matrix material to use. Another reason this epoxy system is chosen is because of its hardener agent Aradur 2954 which has a delayed hardening time. This delayed hardening time is allowed us to complete every mixing and degassing operation before the curing process is started.

2.1.1 Developing The Mold to be Used in Specimen Manufacturing by Soft Molding Method

For pure epoxy specimens, molds are prepared for epoxy/hardener mixture to pour input into an oven together. Silicon molds are prepared with the method of pouring inside of a negative mold made from PMMA. PMMA is chosen because of its smooth surface with the intent of acquiring smooth surfaces silicon molds. PMMA rods with the same diameter as specimens cut with a lathe to a length 2mm longer than the specimens. PMMA rods were then affixed to a rectangular shaped PMMA plate using chloroform. Lastly, four PMMA sheets which are 5mm higher than rods fixed together

to a rectangular shape to enclose rods.

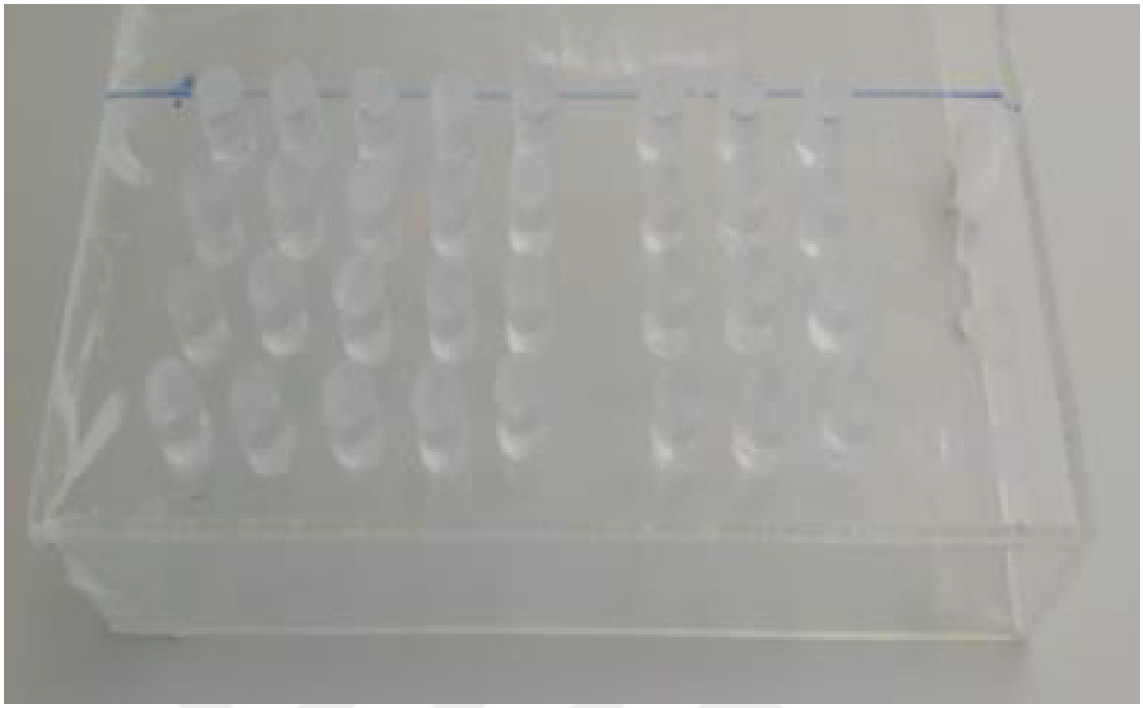


Figure 2.1 PMMA negative mold

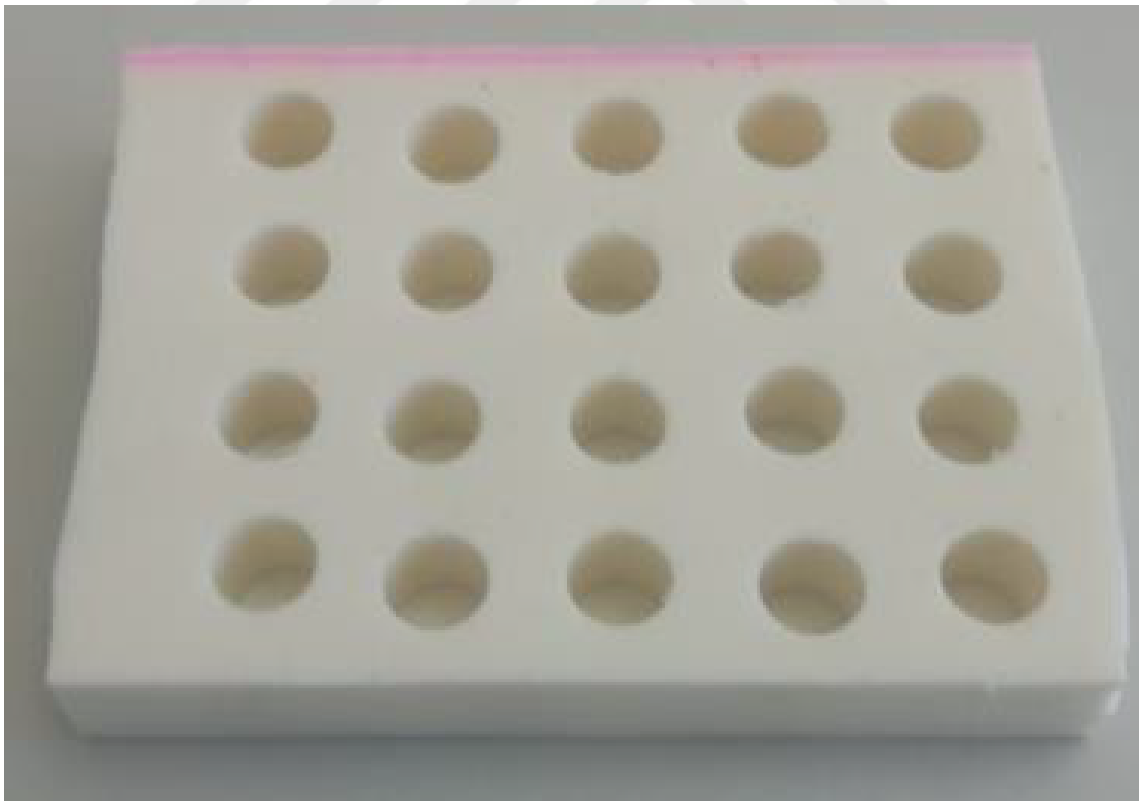


Figure 2.2 Silicon mold prepared for compressive test specimens

RTV2 mold silicone is then poured inside negative mold made from PMMA to make specimen molds. Negative mold designed to hold 20 cylindrical rods and it's reusable.

This way silicon molds to hold 20 specimens can be produced a number of times. RTV2 mold silicon is chosen because of its heat resistance and flexibility so mold can withstand the temperatures oven reaches while epoxies curing process and after the curing, specimens can easily be extracted from the mold.Photographs of the negative mold and the mold are shown in Figures 2.1 and 2.2.

2.1.2 Steps of Production For Pure Epoxy Specimens

Several attempts have been made to produce specimens suitable to conduct experiments with. In the first stages of production effort specimens have had roughness on their surfaces caused by air bubbles trapped inside the mold. With the estimation of rough surfaces (dents and notches shaped like bubbles) on the specimens that can affect negatively mechanical properties, several improvements are made to the production method to obtain smooth-surfaced specimens.

In the first method, epoxy Araldite LY564 and hardener Aradur 2954 mixed with the ratio 100:35 by weight as recommended by the supplier. The amount of epoxy and hardener to use is decided by calculating the volume of one specimen and multiplying that value by the targeted number of specimens and then volume value converted to weight.

- Required epoxy and hardener are weighted using the precision scale with the aforementioned ratio taken into account. Required epoxy and hardener are poured into a beaker.
- Epoxy and hardener mixed using a magnetic stirrer for 15 min at 500 rpm.
- The mixture is then put in a vacuum oven and degassed for 70 min.
- After the degassing process mixture is poured inside the silicone mold and put in an oven for the curing process.
- The mixture is cured in a preheated oven at 80°C for 1h.
- Lastly, the mixture is post-cured at 160°C for 4h.

After these procedures very rough-surfaced specimens has been obtained(Figure 2.3). To improve surface quality several steps are added to the first method:

- Amount of time epoxy and hardener mixture stayed on the magnetic stirrer increased to 20 min and mixing speed increased to 750 rpm.



Figure 2.3 Pure epoxy specimens obtained with the first method

- Instead of the vacuum oven a separate vacuum chamber is used and the mixture is degassed inside the vacuum chamber for 70 min. After the degassing process, it is observed that air bubbles gathered at the top of the mixture.
- Air bubbles which are gathered at the top of the mixture then quickly removed using a flame torch.
- Lastly mixture is molded and cured in the same way as the first method.

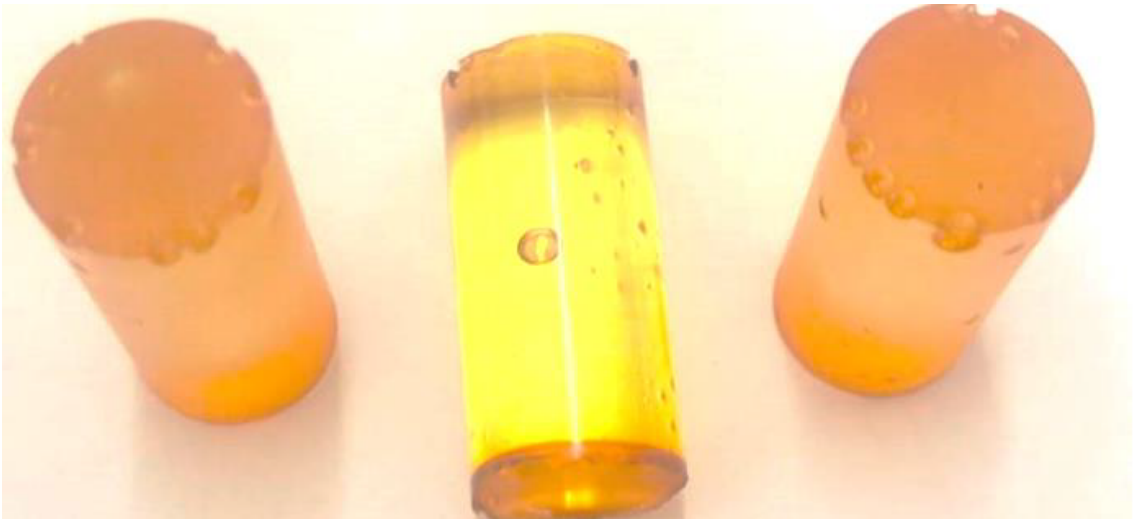


Figure 2.4 Pure epoxy specimens after improvements

After the added steps significant improvement observed in the surface quality (Figure 2.4).

To completely remove the roughness from the side, top, and bottom surfaces improvement effort is continued.

- Amount of time mixture degassed inside vacuum chamber increased to 90min. A flame torch is used to remove gathered air bubbles.
- Mixture then poured inside the silicone mold and degassed for another hour. The remaining air bubbles gathered at the top of the mold were again removed using the flame torch.
- Mixture cured with same methods. Specimens removed from the mold have had smooth surfaces and are in ideal condition to using in experiments (Figure 2.5).



Figure 2.5 Pure epoxy specimens used in experiments

Additionally, the specimen length projected to be 22 mm at the planning stage reduced to be 12mm because of the buckling behavior observed during the first experiments. Buckling problem did not observed after the readjustment of dimensions. Final specimen dimensions are decided as 12 mm in diameter and 12 mm in length for all specimens used in experiments. Specimen dimensions are shown in Figure 2.6 .

2.2 Manufacturing of Graphene-Epoxy Specimens

According to the literature, there are several methods to produce nanocomposites. Mostly used methods to produce nanocomposites are Three Roll Milling (3RM), sonication, high and low shear mixing. Chandrasekaran et.al at 2013 compared these methods to investigate the effects of production methods on the electrical and thermal conductivity, fracture toughness, and storage modulus of the nanocomposites

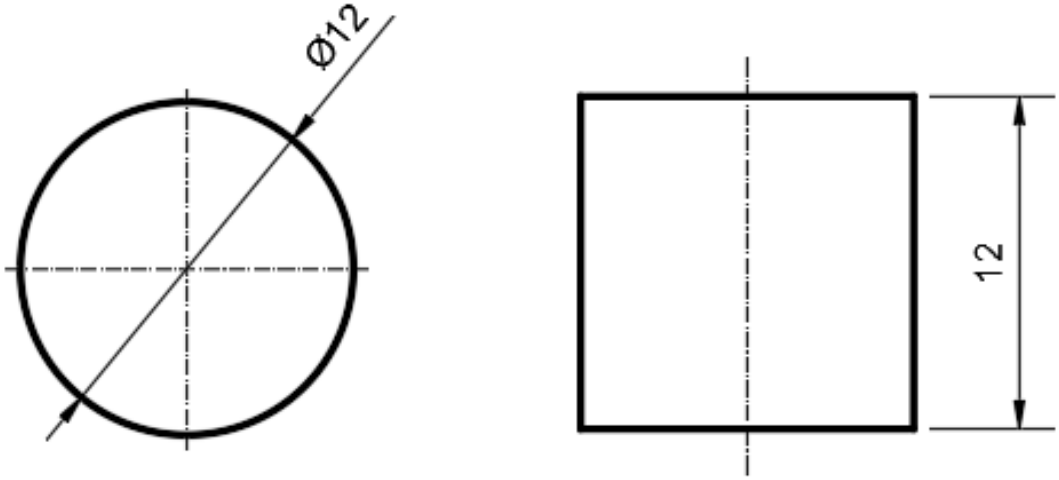


Figure 2.6 Technical drawing showing specimen dimensions

produced. Researchers in their study achieved good dispersion for both methods they have been used but the specimens produced with the 3RM method showed better electrical conductivity. This behavior can be interpreted as the 3RM method has provided better uniform dispersion and exfoliation of graphene. Researchers also in line with this interpretation have decided to complete their research using only 3RM specimens for mechanical and thermal characterization [42]. At another research from Prolongo et. al, high shear mixing and 3RM methods got compared. Researchers produced specimens using 3RM, high shear mixing, and a combination of two methods. In this research specimens produced with the 3RM method and combination, the method is shown similar thermal and mechanical behaviors which are superior to specimens produced with high shear mixing. This case shows us that high shear mixing although provided uniform dispersion failed to exfoliate graphene inside the matrix material. Researchers also recommended the 3RM method instead of high shear mixing while producing nanocomposites [43].

While producing nanocomposites using the 3RM method some unique properties stand out. These are in order of importance: distance between rolls up to 5 μm, rolling speed, and the number of cycles. To determine the best parameters for 3RM to use for the purpose of obtaining specimens with the best material properties a detailed literature review among the research which used the 3RM method is conducted. Gojny et. al in their research have set gap distance (distance between rolls) to 5 μm and observed 12% improvement in Young modulus [44]. Prolongo et. al at their research which they are used graphene 3% by weight set the gap distance to 5 μm and apron speed to 250 rpm and observed 22% improvement in tensile modulus [43]. At another research by Olowojoba et. al gap distance have been set to 5 μm and 13.25% increase have been observed in storage modulus [45]. Lastly Wang et. al set the apron speed

to 250 rpm and observed 48.8% increase in elasticity modulus [46]. Considering this information obtained from the literature review it is decided to set the gap distance to 5 μm and apron speed to 250 rpm for all the specimens to be produced with the 3RM method.

2.2.1 Three Roll Milling Method

3RM method works on the principle of three rolls turning at different speeds and opposite to each other with the intent of creating shear stress. One of the main reasons wanted mechanical properties can not reach while producing graphene-based nano-materials is the agglomeration of graphene flakes inside the matrix material. In this thesis, it is planned to use the three-roll rolling method to prevent the agglomeration of graphene flakes. Three rolls on the device are named feed roll, center roll, and apron roll. While using 3RM paste-like substance is poured between the feed roll and center roll, most of the material accumulates in the area between these rolls. Material that can pass through the rolls is subjected to large shear stresses due to the speed difference between the rolls. Between the center roll and apron roll material is subjected to even larger shear stresses due to the larger speed difference between these rolls. Material gathered from the apron roll is in a state that is properly mixed and free from agglomerations (Figure 2.7). This cycle can be repeated several times to achieve better mixture quality.

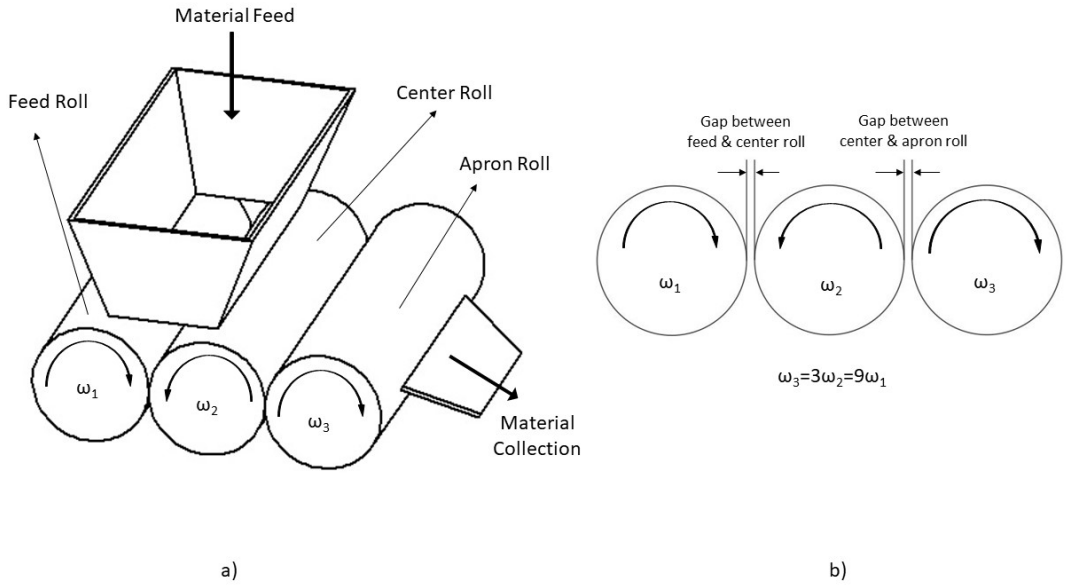


Figure 2.7 a) Three roll milling configuration, b) High shear region between the rolls

For the production of specimens used for the experiments Exakt 80E three roll milling device is used (Figure 2.8).

Based on the results of the experiments conducted with graphene-epoxy specimens produced with 5, 6, 7, and 8 cycles, the optimum number of cycles to use while producing nanocomposites is decided as 5 cycles. The reasoning behind this decision will be discussed in detail in Chapter 3. Again based on the same experiment results lack of improvement in the viscoplastic region is observed. Therefore it is decided to proceed with experimental work with specimens produced with functionalized graphene with the intend of achieving better dispersion and consequently better mechanical properties.



Figure 2.8 Exakt 80E Three Roll Mill device

2.2.2 Functionalization of Graphene

Another problem to overcome while producing nanocomposites with graphene as a reinforcing material is the interface interaction between matrix material and graphene. The reason why interface interaction has a negative effect on the mechanical properties of produced nanocomposites is the agglomeration behavior of graphene caused because of the van der Waals bonds between graphene flakes [47]. In literature, two different methods are used to overcome this effect. The first of these methods is the method of forming covalent bonds between the oxygen

functional groups of graphene. The second method is the method of attaching molecules to graphene flakes with non-covalent bonds. Among the non-covalent functionalization methods, polymer wrapping, surfactant absorption, p-p interaction, and hydrogen bonding are the most widely used [48, 49]. Li et al. non-covalently functionalized graphene using poly (sodium 4-styrenesulfonate)(PSS) and produced nanocomposites using this functionalized graphene and epoxy resin. And the yield strength and modulus of elasticity were improved for the nanocomposite produced [50]. Zhang et al. in their study in which they examined both covalent and non-covalent functionalization methods, an improvement was observed in the mechanical properties of nanocomposites produced with graphene functionalized using Triton X-100 [51]. With the literature review, it was revealed that nanocomposites produced with graphene functionalized using Triton X-100 showed improved mechanical properties [48, 52, 53].

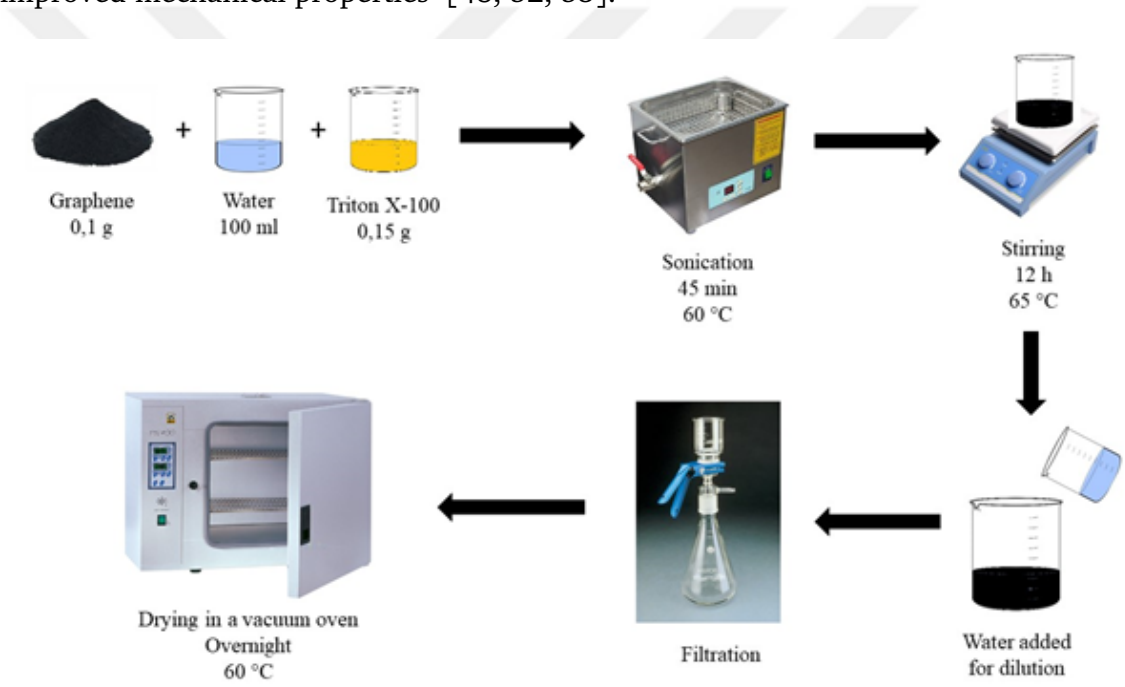


Figure 2.9 Functionalization process of graphene

As a result of the limited studies in the literature on the functionalization of graphene using Triton X-100, the optimum proportional material values to be used were determined [48, 51, 52, 54]. For the functionalization of graphene, first graphene (0.1 g), purified water (100 ml), and triton X-100 (0.15 g) were mixed in a beaker. This mixture was then kept in the sonication bath for 45 min. After sonication, the mixture was stirred for 12 hours at 65 °C with a magnetic stirrer. After mixing, the Triton X-100 – graphene mixture, which was homogeneously mixed, was filtered on the filter paper until only graphene remained. Finally, the filtered graphene was dried in a vacuum oven at 60 °C for 12 hours. The process is shown schematically in Figure 2.9.

2.2.3 Nanocomposite Production

In the production of nanocomposite test specimens, functionalized graphene(f-GNF) and Araldite LY564 epoxy resin / Aradur 2954 hardening agent set produced by Huntsman were used as explained in detail in the previous sections. Appropriate molds from RTV2 mold silicone were produced for the production of the test samples in the desired dimensions. The three-roll rolling method was used to prevent agglomeration of f-GNF inside the epoxy matrix material.

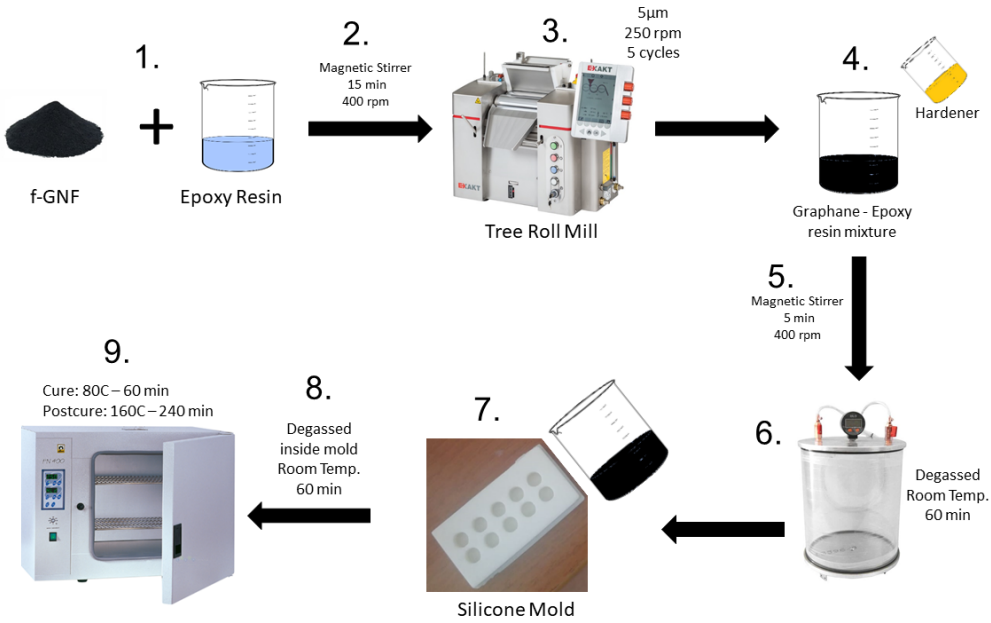


Figure 2.10 Production of nanocomposite specimens using 3RM

While the graphene epoxy mixture is mixed for the production of nanocomposite test specimens and poured into the mold, the gases remaining in the mixture form undesirable air bubbles and roughness after curing. In order to prevent this situation, which reduces the mechanical properties, degassing under vacuum was applied separately after the mixing process and pouring into the mold. The gases in the mixture under vacuum accumulated on the surface of the mixture and then were removed from the mixture using a blowtorch. Finally, graphene epoxy resin and hardener were cured using an oven, according to the manufacturer's recommended temperature and time (Figure 2.10).

The production process steps are given below in substance.

1. Graphene and Araldite 564 epoxy resin were placed in the same beaker at various weight percentages.
2. Graphene and epoxy resin were mixed at 400 rpm for 15 minutes using a magnetic stirrer.

3. The mixture was rolled for 5 cycles by adjusting the distance between the rolls of the 3RM to be 5 μm and the roll rotation speed to be 250 rpm.

4. After the uniform dispersion of f-GNF inside the epoxy matrix, Aradur 2954 hardener was added to the mixture in the ratio recommended by the manufacturer, in a ratio of 100:35.

5. The mixture with added hardener was mixed at 400 rpm for 15 minutes using a magnetic stirrer.

6. The beaker containing the mixture was placed in a vacuum and degassed at room temperature for 60 minutes.

7. After the air bubbles that collected on the upper surface of the mixture was cleaned with a blowtorch, the mixture was poured into a silicone mold.

8. In order to purify the gases that may be trapped in the mixture during pouring, the mold was placed in a vacuum and degassed for 60 minutes.

9. After the air bubbles on the mold was cleaned with a blowtorch, the mold was placed in a preheated oven at 80°C and pre-cured for 60 minutes. At the end of 60 minutes, the oven temperature was increased to 160°C and the curing process was carried out for 240 minutes.

3
CHARACTERIZATION OF GRAPHENE-EPOXY NANOCOMPOSITES

3.1 ARALDITE LY564 Epoxy Compression Test Results

Compression tests were carried out at different strain rates at room temperature with the Instron 5982 universal static test device with a measurement accuracy of +/− 0.5% at YTU Central Laboratory. Specimen diameter is d= 12 mm, length, L= 12 mm. In order to determine the viscoelastic and viscoplastic behavior of the epoxy, compression tests were carried out at 3 different strain rates (0.001, 0.01, and 0.1 /s) until damage. Tests were performed at least 3 times in all conditions and averages were taken. True stress-strain curves are given in Figures 3.1, 3.2 and 3.3.

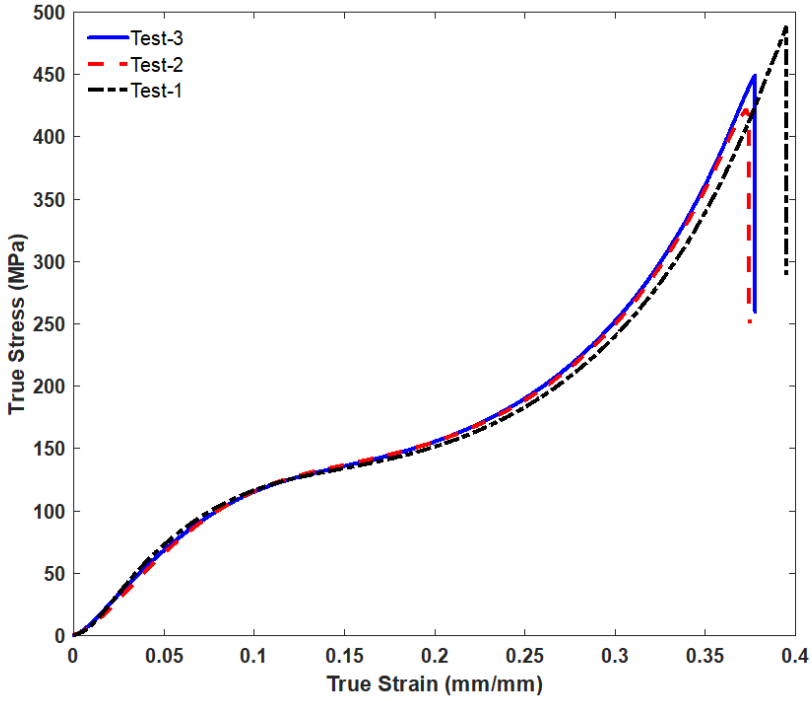


Figure 3.1 Compression test results at strain rate 1.E-3 /s for pure epoxy material (3 test repetitions)

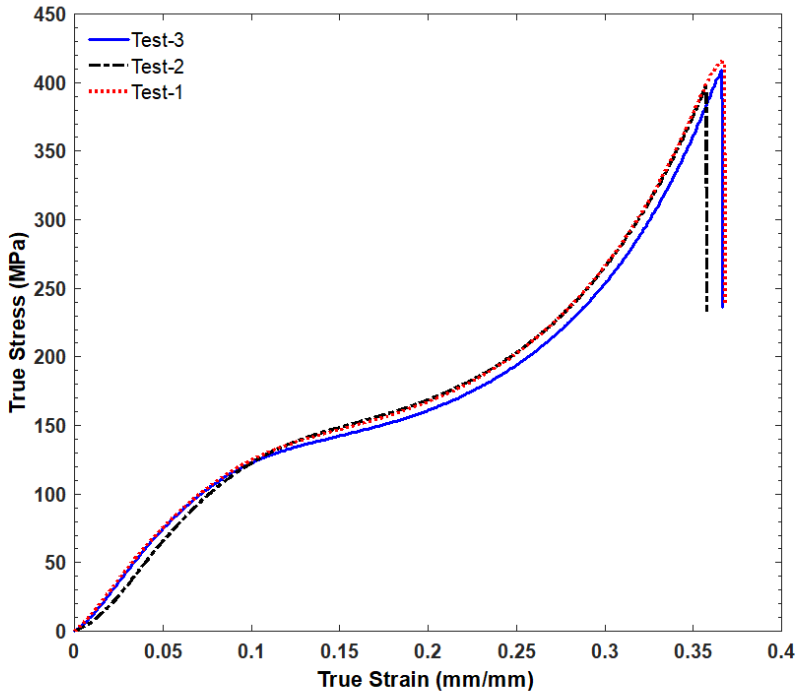


Figure 3.2 Compression test results at strain rate 1.E-2 /s for pure epoxy material (3 test repetitions)

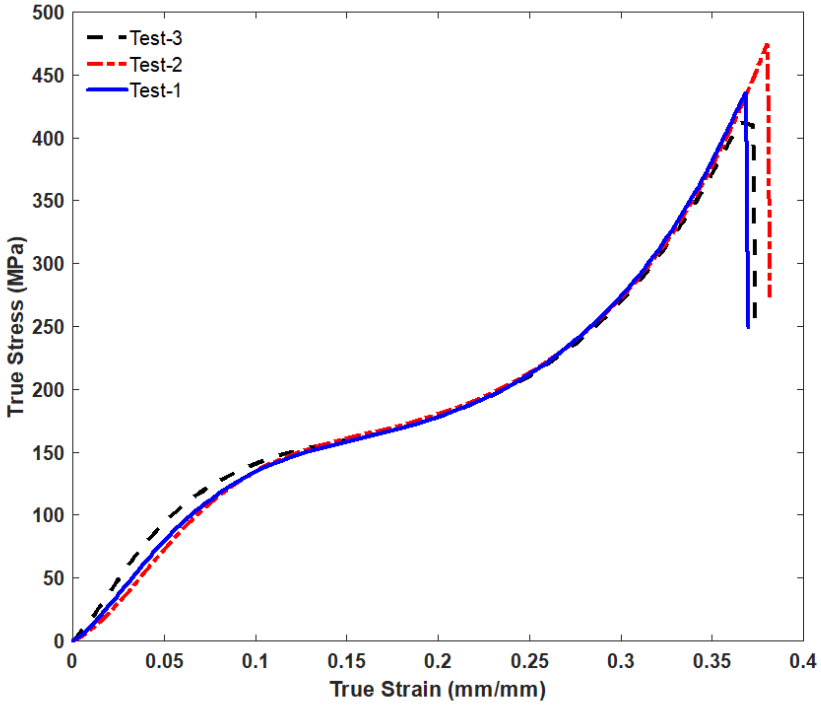


Figure 3.3 Compression test results at strain rate 1.E-1 /s for pure epoxy material (3 test repetitions)

As can be seen in Figure 3.1, 3.2, and 3.3 the compression curves obtained from the repeated tests are almost coincident. This shows that the uncontrollable elements are avoided in the tests, and the tests yield highly reproducible results.

The results obtained by taking the arithmetic averages of the tests performed at each speed are given in Figure 3.4.

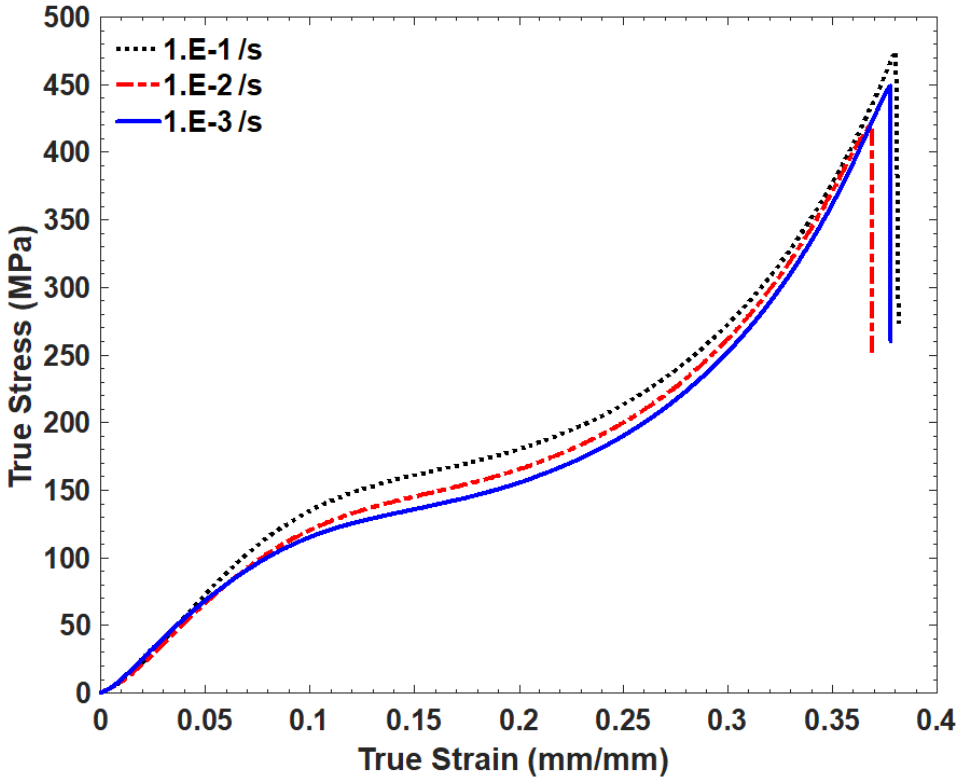


Figure 3.4 True stress-strain response of pure epoxy (Araldite LY564) at three different strain rates (1.E-3, 1.E-2, 1.E-1 /s)

As can be seen from Figure 3.4, the modulus of elasticity and yield stress were increased with increasing strain rate. It is observed that the change in stress with strain increase in pure epoxy specimens is parallel for all strain rates. This change can be summarized as a linear increase in the elastic region, a small non-linear behavior in the yield region, an insignificant strain-softening after the yield region, and a very significant nonlinear hardening that continues until failure. These results seem to be consistent with those in the literature [55].

As will be noticed when the results are examined in more detail, the change in the modulus of elasticity for different strain rates is quite limited. In other words, there is little rate dependency in the elastic region. As it is known, elastic deformation occurs in the form of elastic elongation of the chains as the covalent bonds between the polymer chains reach the chain length in the epoxy and are distorted [45]. The dense

cross-links in Araldite LY 564 strengthen the covalent bonds between the polymer chains and reduce the effect of the strain rate.

While softening and subsequent hardening were observed in most epoxy materials, post-yielding softening behavior was not observed in Araldite LY 564. The material showed hardening behavior without showing softening after yield. A non-linear hardening behavior was observed. The peak point of the transition point from linear to nonlinear is accepted as yield strength [46]. As the tensile value exceeds the yield strength value, the material begins to deform plastically. The plastic deformation here can be explained by the stretching, turning, sliding, and dissolving of the cross-linked chains in the polymer causing permanent deformation. Initially, the chains are highly intertwined; When the tension is high enough, the chains begin to unravel. However, it is observed that there is very little strain softening in the material. From this point onwards, a resistance occurs against continued deformation, and the strength of the specimen increases. With increasing stress, the chains in the epoxy are oriented in the direction of the deformation, and hardening occurs to complete the deformation of the chains. Ultimately, a high-stress value is required for the specimen to break at a certain strain value. It has been determined that this strain range is between 0.36 and 0.4 mm/mm for three different strain rates.

Since the temperature was assumed to be constant (room temperature) in these compression tests, only the effect of strain rate on mechanical properties (modulus of elasticity, yield strength, etc.) was examined. The fact that the mechanical properties are strongly dependent on the temperature and the rate at which the material deforms is due to the viscoelastic, viscoplastic properties of the polymer (epoxy).

The modulus of elasticity was calculated between 0.005 and 0.025 mm/mm strains in the elastic region. The yield strength is calculated as the first point where the $\frac{d\sigma}{d\varepsilon}$ is zero, that is, the linearity ends. Looking at Table 3.1, it is seen that the elastic modulus and yield strength values increase as the strain rate increases. These values only increase as a function of the strain rate (temperature constant up to the yield point). The increase in the mechanical properties here has emerged as a result of the decrease in the mobility of the molecules of the epoxy chains [56].

According to Figure 3.4, although strain hardening occurs at high strains as the strain rate increases, it is seen that the slope of the strain hardening curve decreases as the strain rate increases. It is also seen that ductility increases as the elongation increases. The mechanical properties obtained as a result of the compression test are given in Table 3.1.

Table 3.1 The mechanical properties of Araldite LY 564 epoxy obtained from the quasi-static compression test

Strain Rate (1/s)	Yield Strenth (MPa)	Elasticity Modulus (MPa)	Ultimate Strength (MPa)
1.E−1	137	1987	474
1.E−2	124	1542	420
1.E−3	119	1465	449

3.2 f-GNF - Epoxy Nano-composite Compressive Test Results

Compression tests of nanocomposites were carried out with Instron branded universal static test device with model number 5891 (100 kN capacity) in YTU Central Laboratory at room temperature and under three different strain rates. Specimen diameter and length were determined as 12mm for both dimensions. Since the tests will be performed at three different strain rates as 0.001, 0.01, and 0.1/s, the sample lengths measured before each test were multiplied by the desired strain rate (1/s), and strain rates (mm/s) were determined. The calculated strain rates were entered into the test device. During the experiments, the measurement of the strain and the speed control was made with the crosshead movement of the test device as position controlled. The tests were repeated three times to check the repeatability of the test results for each strain rate.

3.2.1 Determining the Optimum Number of Cycles in 3RM

The three-roll milling procedure shown in Figure 2.10 is used to obtain homogeneous graphene distribution in epoxy. The procedure of running the mixture through the rollers is repeated numerous times to provide improved homogeneity. Investigating the effect of cycle number on mechanical parameters yielded the optimum number of cycles. Initially, the nano-composite generated with varied cycle numbers in 3RM was tested at 1.E-2 /s strain rate to optimize the three roll milling dispersion characteristics. Figure 3.5 shows the real stress-strain curves for various cycle numbers.

As shown in Figure 3.5, the compression behavior of nano-composite materials created with various cycle numbers follows a similar pattern to that of pure epoxy. Compared to the pure epoxy, the material properties (elasticity modulus, yield strength) in the elastic region of the nano-composite specimens (made with 0.1 wt% GNF) were improved. However, it has been discovered that increasing the number of cycles does not result in a significant improvement in the material's mechanical properties. When

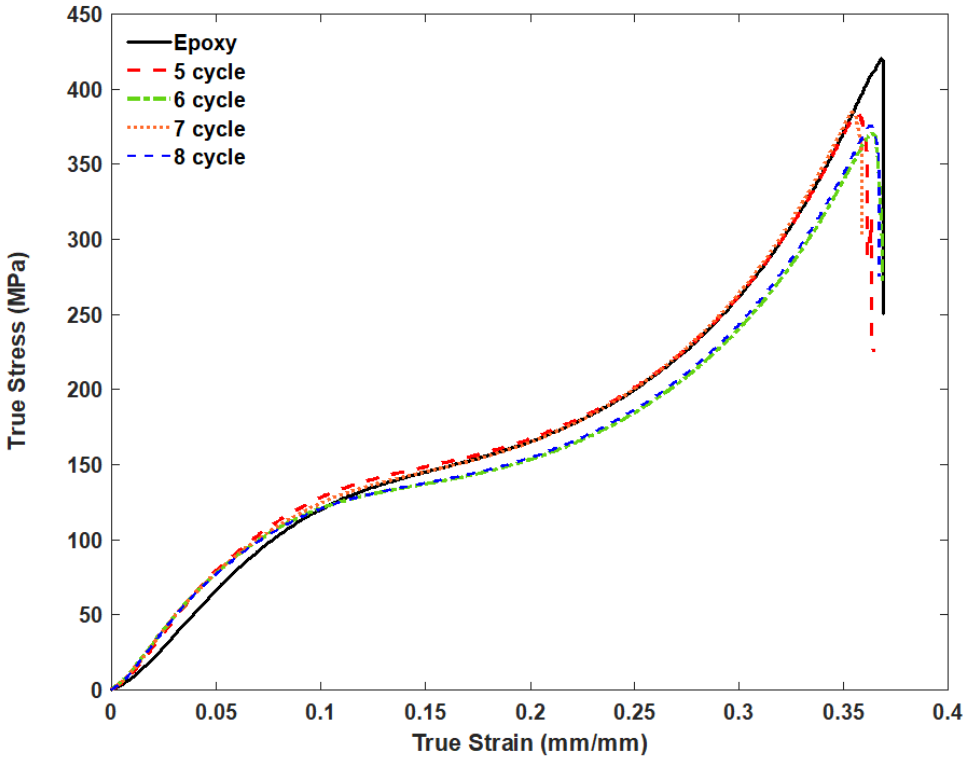


Figure 3.5 The true stress- strain curves under compression for specimens produced with different cycle numbers (Material: GNF- epoxy)

compared to pure epoxy, the material behavior of the nano-composite manufactured in 3RM with five cycles demonstrated an improvement in the elastic region. The material behavior of the specimens manufactured with five cycles was found to be marginally superior to that of samples produced with other cycles (6,7 and 8 cycles). Furthermore, increasing the number of cycles increases both the sample production time and the amount of material waste generated by each new cycle (material remaining on rolls and in used beakers). In light of these circumstances, it was chosen in this work to manufacture nano-composite specimens with five cycles using the 3RM method.

3.2.2 Compression Test Results for Functional Graphene - Epoxy Nano-composite Specimens

Compression test results of 0.1 wt% functionalized graphene (f-GNF) nano-composites under 0.001/s strain rate are given in Figure 3.6. As can be seen from the figure, the compression curves obtained from repeated tests are very close to each other. This shows that the tests give reproducible results. Similarly, three-repeat tests were performed for the other two strain rates, and these tests also gave similar results.

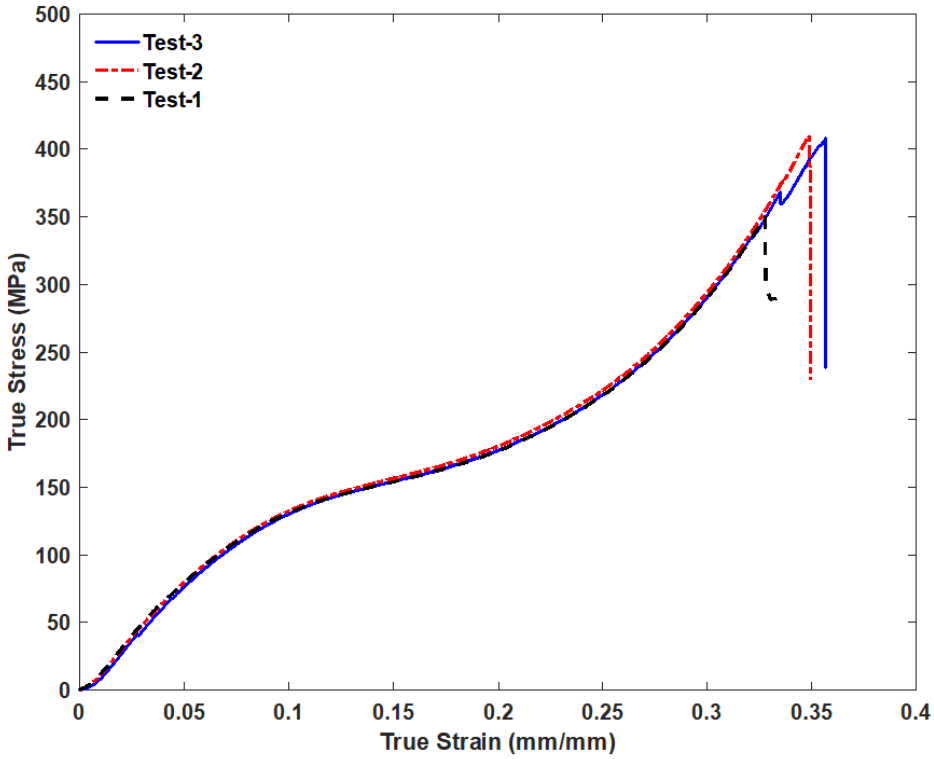


Figure 3.6 Compression tests of 0.1 wt% f-GNF-Epoxy nano-composites at 1.E-3 /s strain rate (3 test repetitions)

Situation in Figure 3.6 is also valid for samples produced using 0.5 wt% of f-GNF. The true stress-strain curves obtained for each strain rate are shown in Figures 3.7 and 3.8, respectively, by taking the arithmetic average of repeated tests of the samples produced with different f-GNF ratios by mass (0.1 and 0.5 wt%).

The pattern of change in material behavior of nanocomposites (containing 0.1 and 0.5 wt % f-GNF) follows a similar trend at all three strain rates, as shown in Figs. 3.7 and 3.8. The elasticity modulus and yield strength of nanocomposite materials increase as the strain rate increases. The slope in the linear region determines elasticity modulus, while the peak point in the region where linearity ends determines yield strength. The viscoelastic region is defined as where the stress-strain curve follows a linear trend until the yield point. The viscoplastic region on the other hand starts after the yield point and continues until the fracture. The viscoplastic region includes rate-dependent behaviors of material that are strain softening and hardening. It can be seen in the viscoelastic region there is a linear increase of the true stress-strain curve starting from the first loading, and rate dependency is minimal in this region. This behavior can be understood by the limited increase in the elasticity modulus. All specimens manufactured with f-GNF and epoxy are shown an insignificant softening behavior after the yield point and a noticeable non-linear hardening after the softening. Rate

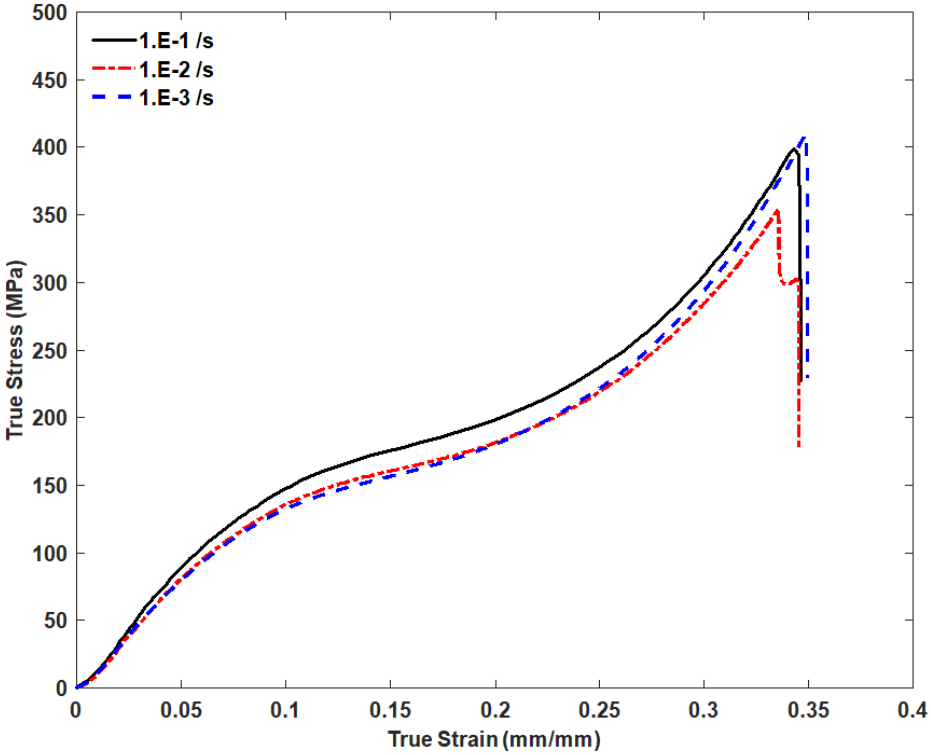


Figure 3.7 True stress-strain curves of f-GNF-epoxy nano-composites with f-GNF content of 0.1 wt% at three different strain rates)

dependency is more evident in the viscoplastic region compared to the viscoelastic region. The improvement in the material properties as the strain rate increases can be explained by the restriction of the movement of the polymer chains that causes a stiffer material response.

The true stress-strain behaviors of f-GNF- epoxy nano-composites with f-GNF content of 0.1 and 0.5 wt % compared to pure epoxy at three different strain rates of 1.E-3, 1.E-2, 1.E-1 /s, are shown in Figs. 3.9, 3.10 and 3.11 respectively.

It has been observed that adding f-GNF into epoxy led to an improvement in material properties for all specimens and strain rates compared to pure epoxy (Figs. 3.9, 3.10 and 3.11). At all strain rates, the elasticity modulus and yield strength values for f-GNF-epoxy nanocomposites containing various amounts of f-GNF increased compared to pure epoxy. Table 3.2 shows the elasticity modulus and yield strength values of pure epoxy (Araldite LY 564) and f-GNF nanocomposites.

According to the literature, improvements in the mechanical properties of nano-composites are restricted to a particular graphene concentration, which is roughly 0.1 wt%, but once this level is exceeded, mechanical properties deteriorate

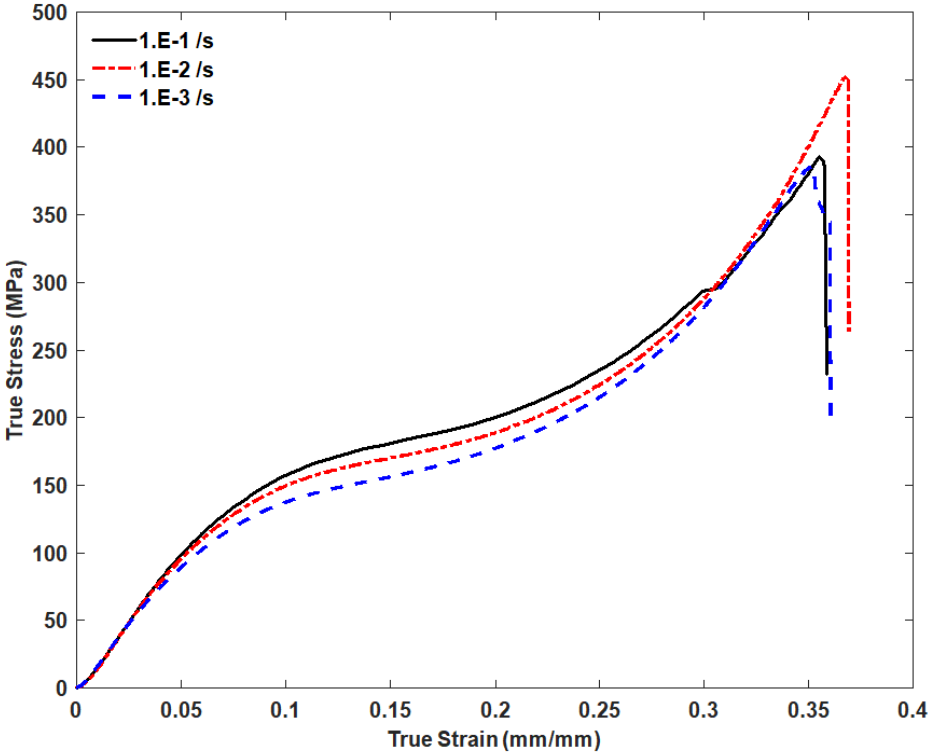


Figure 3.8 True stress-strain curves of f-GNF-epoxy nano-composites with f-GNF content of 0.5 wt % under three different strain rates

Table 3.2 The mechanical properties of Araldite LY 564 epoxy and f-GNF-epoxy nano-composite (0.1 and 0.5 wt% f-GNF) obtained from the quasi-static compression tests

Mechanical Properties	Strain Rate (1/s)	Pure epoxy	f-GNF - epoxy (0.1 wt%)	f-GNF - epoxy (0.5 wt%)
Elasticity Modulus (MPa)	1.E-1	1987	2104	2237
	1.E-2	1542	1899	2171
	1.E-3	1465	1878	2063
Yield strength (MPa)	1.E-1	137	153	162
	1.E-2	124	142	151
	1.E-3	119	134	138

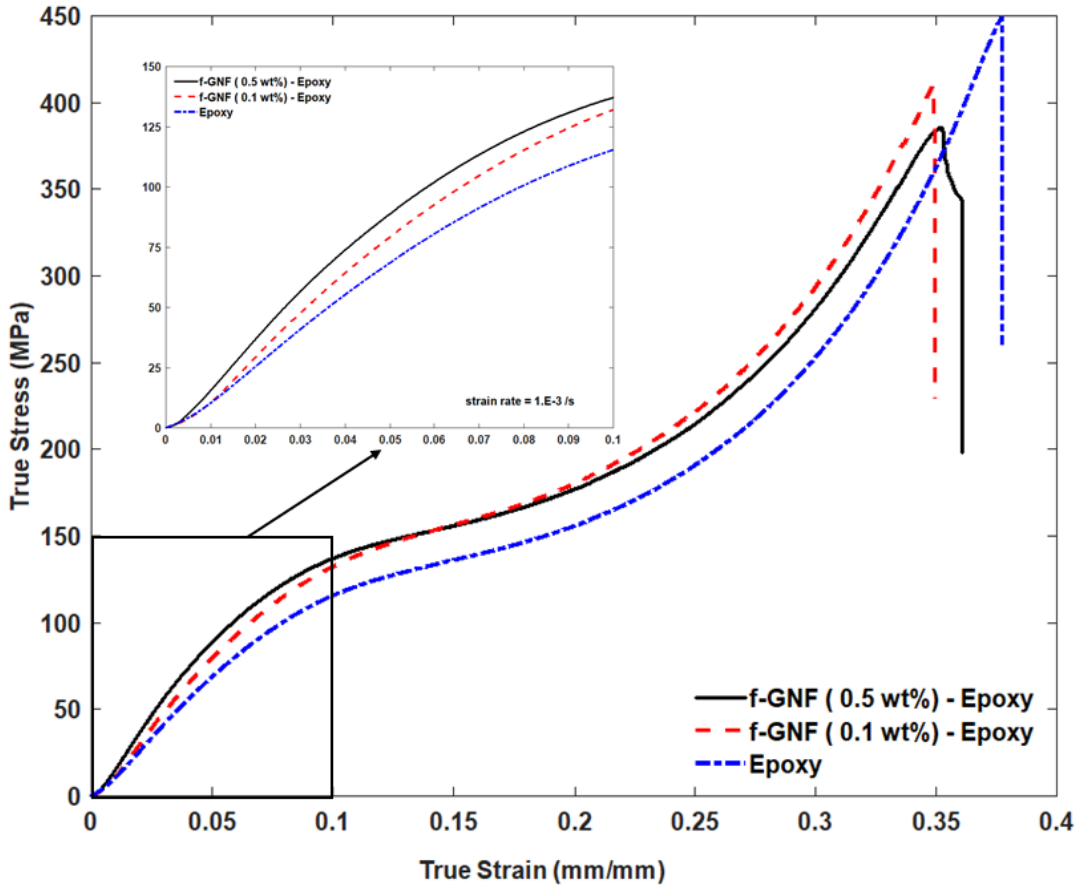


Figure 3.9 Comparison of true stress-strain behaviors of f-GNF-epoxy nanocomposites with f-GNF content of 0.1 and 0.5 wt % with pure epoxy at 1.E-3 /s strain rate.

Table 3.3 The increase in material properties as per centum for different graphene concentrations and strain rates.

Mechanical Properties	Strain Rate (1/s)	Change (%) (0.1 wt% nanocomposite - pure epoxy)	Change (%) (0.5 wt% nanocomposite - pure epoxy)	Change (%) (0. 1wt% nanocomposite - 0.5 wt% nanocomposite)
Elasticity Modulus (MPa)	1.E-1	6	11	6
	1.E-2	19	29	13
	1.E-3	22	29	9
Yield strength (MPa)	1.E-1	10	15	6
	1.E-2	13	18	6
	1.E-3	11	14	3

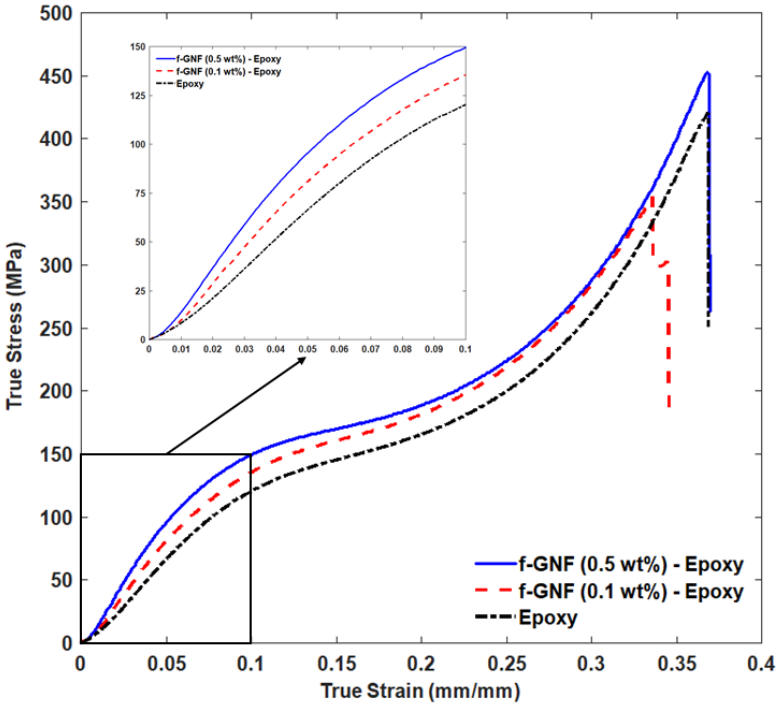


Figure 3.10 Comparison of true stress-strain behaviors of f-GNF-epoxy nanocomposites with f-GNF content of 0.1 and 0.5 wt % with pure epoxy at 1.E-2 /s strain rate.

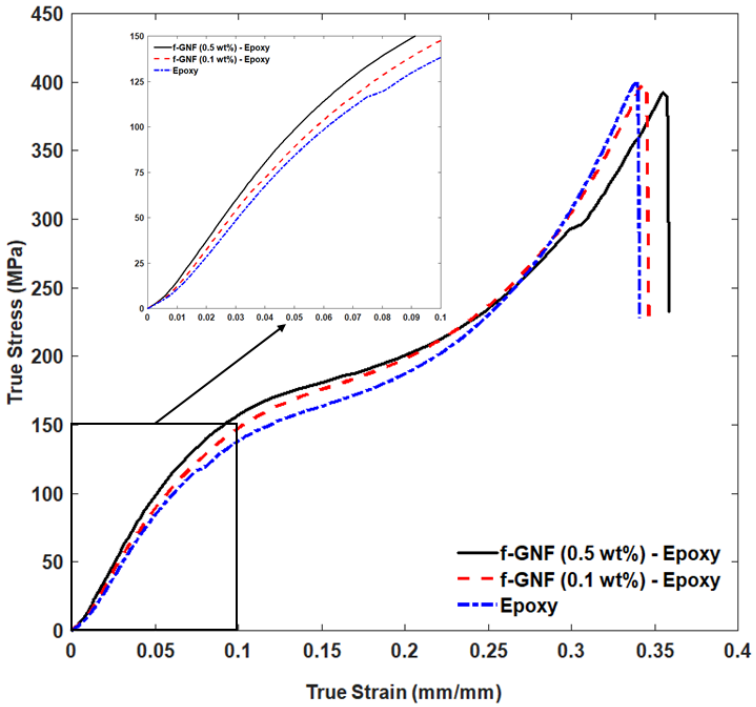


Figure 3.11 Comparison of true stress-strain behaviors of f-GNF-epoxy nanocomposites with f-GNF content of 0.1 and 0.5 wt% with pure epoxy at 1.E-1 /s strain rate.

due to agglomeration issues [57–59]. However, as seen in Figures 3.9, 3.10, 3.11 and Table 3.2, improvements in material properties have continued to climb above this concentration level. This improvement is explained by utilizing the methods of functionalization of graphene with Triton X-100 and effectively dispersing graphene in the epoxy matrix using the 3RM.

The use of a surfactant to functionalize graphene increases its dispersion in the matrix material and allows for efficient interface interaction with the matrix material [53]. In this thesis, hydrophilic and hydrophobic groups in Triton X-100, a non-ionic surfactant, used to functionalize graphene, were found to be beneficial in the homogenous dispersion of graphene by adsorbing onto graphene surfaces [53]. Triton X-100's hydrophilic groups interact with the matrix material via hydrogen bonding and act as a link between graphene and epoxy [59]. As a result, both graphene dispersion and the interface interaction between the matrix material and graphene become more effective. The manufacturing of nanocomposites using the 3RM process is another aspect that improves mechanical properties. By breaking the van der Waals bonds in graphene with the influence of shear stress the agglomeration problem was avoided. As a result, as shown in Tables 3.2 and 3.3, 0.5 wt% f-GNF composites show the greatest improvement in both elasticity modulus and yield strength when compared to pure epoxy at all strain rates.

4
RESULTS AND DISCUSSIONS

In this study, the optimum method for the manufacturing of graphene-epoxy nanocomposite was determined and the mechanical properties of the nanocomposite specimens produced with this method were characterized by conducting compression tests. Graphene functionalized using Triton X-100 surfactant was homogeneously dispersed in epoxy using the 3RM device. Specimens containing 0.1 and 0.5 wt% graphene were manufactured and subjected to compression tests at strain rates of 1.E-3, 1.E-2, and 1.E-1 /s. Thus, the effect of graphene amount and strain rate on the mechanical properties of the manufactured nanocomposite specimens was determined.

A hybrid method has been developed in which 3RM and functionalization methods are used together as a manufacturing method. First of all, the functionalization process was carried out by using Triton X-100 surfactant to prevent the graphene particles from forming van der Waals bonds between each other and causing agglomerations. The f-GNF obtained after the functionalization process was homogeneously dispersed in epoxy using the 3RM device. The 3RM device exposed the epoxy and f-GNF mixture passing between its rollers to high shear stresses and broke the van der Waals bonds that may still occur between the f-GNFs, allowing f-GNF and epoxy to mix homogeneously.

After the manufacturing method was determined, the characterization phase of the produced specimens was started. First, pure epoxy specimens were manufactured and compression tests were carried out. Compression tests were conducted at three different strain rates considering the time-dependent behavior of the epoxy(1.E-3, 1.E-2, and 1.E-1 /s). At the strain rates of 1.E-1, 1.E-2, and 1.E-3 /s, the elasticity modulus of the pure epoxy specimens manufactured as the control group were determined as 1987, 1542, and 1456 MPa, respectively, and the yield strengths were determined as 137, 124, and 119 MPa, respectively. In parallel with the literature, it has been observed that the mechanical properties increase as the strain rate increases. Compression tests on pure epoxy specimens were repeated three times,

thus confirming the repeatability of the tests.

After the characterization of the mechanical properties of the pure epoxy specimens manufactured to be used as the control group was completed, the characterization of the mechanical properties of the nanocomposite specimens was started. Specimens containing 0.1 and 0.5 wt% f-GNF were manufactured and compression tests were performed on these specimens. The tests were performed at three different strain rates and in triplicate, as in pure epoxy specimens. The results of compression tests performed at different strain rates are as follows:

- As a result of the compression tests performed at 1.E-1 /s strain rate, the elasticity modulus of the specimens containing 0.1 wt% f-GNF was determined to be 2104 MPa, and the elasticity modulus of the specimens containing 0.5 wt% f-GNF was found to be 2237 MPa. At the same strain rate, the yield strength of 0.1 wt% specimens was calculated as 153 MPa and the yield strength of 0.5 wt% specimens was calculated as 162 MPa.
- As a result of the compression tests performed at 1.E-2 /s strain rate, the elasticity modulus and yield strength values of the specimens containing 0.1 wt% f-GNF were determined as 1899 and 142 MPa, respectively. And the elasticity modulus and yield strength values of the samples containing 0.5 wt% f-GNF were determined as 2171 and 151 MPa, respectively.
- In the experiments carried out at 1.E-3 /s strain rate, the elasticity modulus values for the specimens containing 0.1 and 0.5 wt% f-GNF were determined as 1878 and 2063 MPa, respectively, and the yield strength values were determined as 134 and 138 MPa, respectively.

When the specimens produced using 0.1 wt% graphene are compared with the pure epoxy specimens, an increase of up to 22% in the elasticity modulus and up to 13% in the yield strength was observed. This proves that the graphene reinforcement leads to an increase in the mechanical properties of the epoxy.

In the literature, it has been reported that the use of graphene reinforcement with more than 0.1 wt% graphene causes a decrease in mechanical properties due to agglomeration problems. However, between the samples produced with 0.1 and 0.5 wt% f-GNF, an increase of up to 13% in the elasticity modulus and up to 6% in the yield strength was observed. This proves that the developed production method solves the agglomeration problem and that a further increase in mechanical properties can be achieved with more graphene reinforcement. The production method is also

environmentally friendly, as it does not contain chemical solvents that are harmful to health and the environment, and is suitable not only for the laboratory environment, but also for large-scale nanocomposite production.

REFERENCES

[1] A. A. Balandin, S. Ghosh, W. Bao, I. Calizo, D. Teweldebrhan, F. Miao, C. N. Lau, "Superior thermal conductivity of single-layer graphene," *Nano letters*, vol. 8, no. 3, pp. 902–907, 2008.

[2] H. Mehdipour, K. Ostrikov, A. E. Rider, Z. Han, "Heating and plasma sheath effects in low-temperature, plasma-assisted growth of carbon nanofibers," *Plasma Processes and Polymers*, vol. 8, no. 5, pp. 386–400, 2011.

[3] K. S. Novoselov, A. K. Geim, S. V. Morozov, D.-e. Jiang, Y. Zhang, S. V. Dubonos, I. V. Grigorieva, A. A. Firsov, "Electric field effect in atomically thin carbon films," *science*, vol. 306, no. 5696, pp. 666–669, 2004.

[4] B. Lang, "A leed study of the deposition of carbon on platinum crystal surfaces," *Surface Science*, vol. 53, no. 1, pp. 317–329, 1975.

[5] X. Liang, A. S. Chang, Y. Zhang, B. D. Harteneck, H. Choo, D. L. Olynick, S. Cabrini, "Electrostatic force assisted exfoliation of prepatterned few-layer graphenes into device sites," *Nano letters*, vol. 9, no. 1, pp. 467–472, 2009.

[6] L. Ci, L. Song, D. Jariwala, A. L. Elıas, W. Gao, M. Terrones, P. M. Ajayan, "Graphene shape control by multistage cutting and transfer," *Advanced Materials*, vol. 21, no. 44, pp. 4487–4491, 2009.

[7] L. M. Viculis, J. J. Mack, O. M. Mayer, H. T. Hahn, R. B. Kaner, "Intercalation and exfoliation routes to graphite nanoplatelets," *Journal of Materials Chemistry*, vol. 15, no. 9, pp. 974–978, 2005.

[8] S. Das, P. Sudhagar, Y. S. Kang, W. Choi, "Synthesis and characterization of graphene," *Carbon Nanomaterials for Advanced Energy Systems: Advances in Materials Synthesis and Device Applications*, pp. 85–131, 2015.

[9] M. S. A. Bhuyan, M. N. Uddin, M. M. Islam, F. A. Bipasha, S. S. Hossain, "Synthesis of graphene," *International Nano Letters*, vol. 6, no. 2, pp. 65–83, 2016.

[10] Z.-Y. Juang, C.-Y. Wu, C.-W. Lo, W.-Y. Chen, C.-F. Huang, J.-C. Hwang, F.-R. Chen, K.-C. Leou, C.-H. Tsai, "Synthesis of graphene on silicon carbide substrates at low temperature," *Carbon*, vol. 47, no. 8, pp. 2026–2031, 2009.

[11] D. Wei, Y. Liu, Y. Wang, H. Zhang, L. Huang, G. Yu, "Synthesis of n-doped graphene by chemical vapor deposition and its electrical properties," *Nano letters*, vol. 9, no. 5, pp. 1752–1758, 2009.

[12] A. Reina, X. Jia, J. Ho, D. Nezich, H. Son, V. Bulovic, M. S. Dresselhaus, J. Kong, "Large area, few-layer graphene films on arbitrary substrates by chemical vapor deposition," *Nano letters*, vol. 9, no. 1, pp. 30–35, 2009.

[13] X. Li, W. Cai, J. An, S. Kim, J. Nah, D. Yang, R. Piner, A. Velamakanni, I. Jung, E. Tutuc, S. K. Banerjee, L. Colombo, R. S. Ruoff, "Large-area synthesis of high-quality and uniform graphene films on copper foils," *science*, vol. 324, no. 5932, pp. 1312–1314, 2009.

[14] K. Subrahmanyam, L. Panchakarla, A. Govindaraj, C. Rao, "Simple method of preparing graphene flakes by an arc-discharge method," *The Journal of Physical Chemistry C*, vol. 113, no. 11, pp. 4257–4259, 2009.

[15] K. Subrahmanyam, S. Vivekchand, A. Govindaraj, C. Rao, "A study of graphenes prepared by different methods: Characterization, properties and solubilization," *Journal of Materials Chemistry*, vol. 18, no. 13, pp. 1517–1523, 2008.

[16] M. D. Stoller, S. Park, Y. Zhu, J. An, R. S. Ruoff, "Graphene-based ultracapacitors," *Nano letters*, vol. 8, no. 10, pp. 3498–3502, 2008.

[17] L. Panchakarla, K. Subrahmanyam, S. Saha, A. Govindaraj, H. Krishnamurthy, U. Waghmare, C. Rao, "Synthesis, structure, and properties of boron-and nitrogen-doped graphene," *Advanced Materials*, vol. 21, no. 46, pp. 4726–4730, 2009.

[18] L. Ci, L. Song, C. Jin, D. Jariwala, D. Wu, Y. Li, A. Srivastava, Z. Wang, K. Storr, L. Balicas, F. Liu, P. M. Ajayan, "Atomic layers of hybridized boron nitride and graphene domains," *Nature materials*, vol. 9, no. 5, pp. 430–435, 2010.

[19] F.-L. Jin, S.-J. Park, "Thermal properties and toughness performance of hyperbranched-polyimide-modified epoxy resins," *Journal of Polymer Science Part B: Polymer Physics*, vol. 44, no. 23, pp. 3348–3356, 2006.

[20] F.-L. Jin, C.-J. Ma, S.-J. Park, "Thermal and mechanical interfacial properties of epoxy composites based on functionalized carbon nanotubes," *Materials Science and Engineering: A*, vol. 528, no. 29-30, pp. 8517–8522, 2011.

[21] W. Liu, Z. Wang, "Silicon-containing cycloaliphatic epoxy resins with systematically varied functionalities: Synthesis and structure/property relationships," *Macromolecular Chemistry and Physics*, vol. 212, no. 9, pp. 926–936, 2011.

[22] M. J. Yoo, S. H. Kim, S. D. Park, W. S. Lee, J.-W. Sun, J.-H. Choi, S. Nahm, "Investigation of curing kinetics of various cycloaliphatic epoxy resins using dynamic thermal analysis," *European Polymer Journal*, vol. 46, no. 5, pp. 1158–1162, 2010.

[23] S.-J. Park, T.-J. Kim, J.-R. Lee, "Cure behavior of diglycidylether of bisphenol a/trimethylolpropane triglycidylether epoxy blends initiated by thermal latent catalyst," *Journal of Polymer Science Part B: Polymer Physics*, vol. 38, no. 16, pp. 2114–2123, 2000.

[24] G.-H. Kwak, S.-J. Park, J.-R. Lee, "Thermal stability and mechanical behavior of cycloaliphatic–dgeba epoxy blend system initiated by cationic latent catalyst," *Journal of applied polymer science*, vol. 78, no. 2, pp. 290–297, 2000.

[25] M.-C. Lee, T.-H. Ho, C.-S. Wang, "Synthesis of tetrafunctional epoxy resins and their modification with polydimethylsiloxane for electronic application," *Journal of Applied Polymer Science*, vol. 62, no. 1, pp. 217–225, 1996.

[26] B. Guo, D. Jia, W. Fu, Q. Qiu, "Hygrothermal stability of dicyanate-novolac epoxy resin blends," *Polymer degradation and stability*, vol. 79, no. 3, pp. 521–528, 2003.

[27] M. Stemmelen, F. Pessel, V. Lapinte, S. Caillol, J.-P. Habas, J.-J. Robin, "A fully biobased epoxy resin from vegetable oils: From the synthesis of the precursors by thiol-ene reaction to the study of the final material," *Journal of Polymer Science Part A: Polymer Chemistry*, vol. 49, no. 11, pp. 2434–2444, 2011.

[28] H. Nouailhas, C. Aouf, C. Le Guernevé, S. Caillol, B. Boutevin, H. Fulcrand, "Synthesis and properties of biobased epoxy resins. part 1. glycidylation of flavonoids by epichlorohydrin," *Journal of Polymer Science Part A: Polymer Chemistry*, vol. 49, no. 10, pp. 2261–2270, 2011.

[29] W. Zhang, X. Li, R. Yang, "Pyrolysis and fire behaviour of epoxy resin composites based on a phosphorus-containing polyhedral oligomeric silsesquioxane (dopo-poss)," *Polymer degradation and stability*, vol. 96, no. 10, pp. 1821–1832, 2011.

[30] X. Wang, Q. Zhang, "Synthesis, characterization, and cure properties of phosphorus-containing epoxy resins for flame retardance," *European Polymer Journal*, vol. 40, no. 2, pp. 385–395, 2004.

[31] A. Gergely, I. Bertóti, T. Török, É. Pfeifer, E. Kálmán, "Corrosion protection with zinc-rich epoxy paint coatings embedded with various amounts of highly dispersed polypyrrole-deposited alumina monohydrate particles," *Progress in Organic Coatings*, vol. 76, no. 1, pp. 17–32, 2013.

[32] Y. Hao, F. Liu, E.-H. Han, "Protection of epoxy coatings containing polyaniline modified ultra-short glass fibers," *Progress in Organic Coatings*, vol. 76, no. 4, pp. 571–580, 2013.

[33] M. Shamsuddoha, M. M. Islam, T. Aravinthan, A. Manalo, K.-t. Lau, "Characterisation of mechanical and thermal properties of epoxy grouts for composite repair of steel pipelines," *Materials & Design (1980-2015)*, vol. 52, pp. 315–327, 2013.

[34] K. Ahmed, S. S. Nizami, N. Z. Raza, "Characteristics of natural rubber hybrid composites based on marble sludge/carbon black and marble sludge/rice husk derived silica," *Journal of Industrial and Engineering Chemistry*, vol. 19, no. 4, pp. 1169–1176, 2013.

[35] M. M. Ayad, A. A. El-Nasr, J. Stejskal, "Kinetics and isotherm studies of methylene blue adsorption onto polyaniline nanotubes base/silica composite," *Journal of Industrial and Engineering Chemistry*, vol. 18, no. 6, pp. 1964–1969, 2012.

[36] A. A. Azeez, K. Y. Rhee, S. J. Park, D. Hui, "Epoxy clay nanocomposites–processing, properties and applications: A review," *Composites Part B: Engineering*, vol. 45, no. 1, pp. 308–320, 2013.

[37] X. Li, P. Bandyopadhyay, T. Kshetri, N. H. Kim, J. H. Lee, "Novel hydroxylated boron nitride functionalized p-phenylenediamine-grafted graphene: An excellent filler for enhancing the barrier properties of polyurethane," *Journal of Materials Chemistry A*, vol. 6, no. 43, pp. 21 501–21 515, 2018.

[38] J. Ding, H. Zhao, D. Ji, B. Xu, X. Zhao, Z. Wang, D. Wang, Q. Zhou, H. Yu, "Achieving long-term anticorrosion via the inhibition of graphene's electrical activity," *Journal of Materials Chemistry A*, vol. 7, no. 6, pp. 2864–2874, 2019.

[39] R. Scaffaro, L. Botta, A. Maio, G. Gallo, "Pla graphene nanoplatelets nanocomposites: Physical properties and release kinetics of an antimicrobial agent," *Composites Part B: Engineering*, vol. 109, pp. 138–146, 2017.

[40] E.-C. Cho, J.-H. Huang, C.-P. Li, C.-W. Chang-Jian, K.-C. Lee, Y.-S. Hsiao, J.-H. Huang, "Graphene-based thermoplastic composites and their application for led thermal management," *Carbon*, vol. 102, pp. 66–73, 2016.

[41] S. Qin, C. Chen, M. Cui, A. Zhang, H. Zhao, L. Wang, "Facile preparation of polyimide/graphene nanocomposites via an in situ polymerization approach," *Rsc Advances*, vol. 7, no. 5, pp. 3003–3011, 2017.

[42] S. Chandrasekaran, C. Seidel, K. Schulte, "Preparation and characterization of graphite nano-platelet (gnp)/epoxy nano-composite: Mechanical, electrical and thermal properties," *European Polymer Journal*, vol. 49, no. 12, pp. 3878–3888, 2013.

[43] S. Prolongo, A. Jimenez-Suarez, R. Moriche, A. Ureña, "In situ processing of epoxy composites reinforced with graphene nanoplatelets," *Composites Science and Technology*, vol. 86, pp. 185–191, 2013.

[44] F. Gojny, M. Wichmann, U. Köpke, B. Fiedler, K. Schulte, "Carbon nanotube-reinforced epoxy-composites: Enhanced stiffness and fracture toughness at low nanotube content," *Composites science and technology*, vol. 64, no. 15, pp. 2363–2371, 2004.

[45] G. B. Olowojoba, S. Eslava, E. S. Gutierrez, A. J. Kinloch, C. Mattevi, V. G. Rocha, A. C. Taylor, "In situ thermally reduced graphene oxide/epoxy composites: Thermal and mechanical properties," *Applied nanoscience*, vol. 6, no. 7, pp. 1015–1022, 2016.

[46] F. Wang, L. T. Drzal, Y. Qin, Z. Huang, "Mechanical properties and thermal conductivity of graphene nanoplatelet/epoxy composites," *Journal of materials science*, vol. 50, no. 3, pp. 1082–1093, 2015.

[47] M. J. McAllister, J.-L. Li, D. H. Adamson, H. C. Schniepp, A. A. Abdala, J. Liu, M. Herrera-Alonso, D. L. Milius, R. Car, R. K. Prud'homme, I. A. Aksay, "Single sheet functionalized graphene by oxidation and thermal expansion of graphite," *Chemistry of materials*, vol. 19, no. 18, pp. 4396–4404, 2007.

[48] J. Dai, C. Peng, F. Wang, G. Zhang, Z. Huang, "Effects of functionalized graphene nanoplatelets on the morphology and properties of phenolic resins," *Journal of Nanomaterials*, vol. 2016, 2016.

[49] V. Georgakilas, J. N. Tiwari, K. C. Kemp, J. A. Perman, A. B. Bourlinos, K. S. Kim, R. Zboril, "Noncovalent functionalization of graphene and graphene oxide for energy materials, biosensing, catalytic, and biomedical applications," *Chemical reviews*, vol. 116, no. 9, pp. 5464–5519, 2016.

[50] Y. Li, J. Tang, L. Huang, Y. Wang, J. Liu, X. Ge, S. C. Tjong, R. K. Y. Li, L. A. Belfiore, "Facile preparation, characterization and performance of noncovalently functionalized graphene/epoxy nanocomposites with poly (sodium 4-styrenesulfonate)," *Composites Part A: Applied Science and Manufacturing*, vol. 68, pp. 1–9, 2015.

[51] G. Zhang, F. Wang, J. Dai, Z. Huang, "Effect of functionalization of graphene nanoplatelets on the mechanical and thermal properties of silicone rubber composites," *Materials*, vol. 9, no. 2, p. 92, 2016.

[52] M. A. Anwer, J. Wang, H. E. Naguib, "1d/2d cnf/gnp hybrid nanofillers: Evaluation of the effect of surfactant on the morphological, mechanical, fracture, and thermal characteristics of their nanocomposites with epoxy resin," *Industrial & Engineering Chemistry Research*, vol. 58, no. 19, pp. 8131–8139, 2019.

[53] Y.-J. Wan, L.-C. Tang, D. Yan, L. Zhao, Y.-B. Li, L.-B. Wu, J.-X. Jiang, G.-Q. Lai, "Improved dispersion and interface in the graphene/epoxy composites via a facile surfactant-assisted process," *Composites science and technology*, vol. 82, pp. 60–68, 2013.

[54] O. A. Hussein, K. Habib, R. Saidur, A. S. Muhsan, S. Shahabuddin, O. A. Alawi, "The influence of covalent and non-covalent functionalization of gnp based nanofluids on its thermophysical, rheological and suspension stability properties," *RSC Advances*, vol. 9, no. 66, pp. 38 576–38 589, 2019.

[55] R.-M. Wang, S.-R. Zheng, Y.-P. G. Zheng, *Polymer matrix composites and technology*. Elsevier, 2011.

[56] S. Shadlou, B. Ahmadi-Moghadam, F. Taheri, "The effect of strain-rate on the tensile and compressive behavior of graphene reinforced epoxy/nanocomposites," *Materials & Design*, vol. 59, pp. 439–447, 2014.

[57] A. Acar, Ö. Ü. Çolak, D. Uzunsoy, "Synthesis and characterization of graphene-epoxy nanocomposites," *Materials Testing*, vol. 57, no. 11-12, pp. 1001–1005, 2015.

[58] Ö. U. Colak, N. Bahlouli, D. Uzunsoy, C. Francart, "High strain rate behavior of graphene-epoxy nanocomposites," *Polymer Testing*, vol. 81, p. 106 219, 2020.

[59] Q.-A. Poutrel, Z. Wang, D. Wang, C. Soutis, M. Gresil, "Effect of pre and post-dispersion on electro-thermo-mechanical properties of a graphene enhanced epoxy," *Applied Composite Materials*, vol. 24, no. 2, pp. 313–336, 2017.

PUBLICATIONS FROM THE THESIS

Papers

1. O. Bakbak, B. E. Birkan, A. Acar, ve O. Colak, “Mechanical characterization of Araldite LY 564 epoxy: creep, relaxation, quasi-static compression and high strain rate behaviors”, Polym. Bull., Mar. 2021, doi: 10.1007/s00289-021-03624-x.

2. O. Colak, B. E. Birkan, O. Bakbak, A. Acar.,D. Uzunsoy, "Functionalized Graphene-Epoxy Nanocomposites: Experimental Investigation of Viscoelastic and Viscoplastic Behaviors," Mech. Time-Depend Mater., 2021, (Accepted)

Conference Papers

1. B. E. Birkan, O. Bakbak, A. Acar, O. Colak, "Three Roll Milling for Manufacturing of Graphene- Epoxy Nanocomposites", ICAME 2021, ss.925-929, ISBN : 978-975-461-599-9, 2021